Fuel Cell Power Plant Integrated Systems Evaluation

EM-1097
Research Project 1085-1

Interim Report, June 1979

Prepared by

GENERAL ELECTRIC COMPANY
Energy Systems Program Department
One River Road
Schenectady, New York 12345

Principal Investigators
T. L. Bonds
M. H. Dawes
R. Roberts
A. W. Schnacke
L. W. Spradlin

Prepared for

Electric Power Research Institute
3412 Hillview Avenue
Palo Alto, California 94304

EPRI Project Manager
A. P. Fickett
Fossil Fuel and Advanced Systems Division

ORDERING INFORMATION

Requests for copies of this report should be directed to Research Reports Center (RRC), Box 10090, Palo Alto, CA 94303, (415) 961-9043. There is no charge for reports requested by EPRI member utilities and affiliates, contributing nonmembers, U.S. utility associations, U.S. government agencies (federal, state, and local), media, and foreign organizations with which EPRI has an information exchange agreement. On request, RRC will send a catalog of EPRI reports.

NOTICE

This report was prepared by the organization(s) named below as an account of work sponsored by the Electric Power Research Institute, Inc. (EPRI). Neither EPRI, members of EPRI, the organization(s) named below, nor any person acting on their behalf: (a) makes any warranty or representation, express or implied, with respect to the accuracy, completeness, or usefulness of the information contained in this report, or that the use of any information, apparatus, method, or process disclosed in this report may not infringe privately owned rights; or (b) assumes any liabilities with respect to the use of, or for damages resulting from the use of, any information, apparatus, method, or process disclosed in this report.

Prepared by
General Electric Company
Schenectady, New York

ABSTRACT

Molten carbonate fuel cell power plants are candidates for two future utility applications. One application would be as small dispersed generators using liquid or gaseous fuels. The other would be as central station power plants fueled by coal.

This interim report describes the activities conducted to develop and analyze molten carbonate fuel cell power plant design configurations for these two applications. It considers both small (5 MW) dispersed, oil-fueled and large (675 MW) coal-fueled power plants.

Plant requirements have been established and they include a heat rate of 7500 Btu/kWh for the oil-fueled plant and 6800 Btu/kWh for the coal-fueled plant.

Described are the activities that will lead to the selection of a reference power plant design for each of the power plant types. These reference cycles will form the basis for assessments directed at economic evaluations and trade-offs designed to further improve and detail the plants.

Plant design guidelines and the analytical methodologies developed in the course of this program are presented.

Seven coal-fueled and one oil-fueled plant configurations are identified and discussed. Three of the coal-fueled cases meet the heat rate goal. The oil-fueled case calculates to a 7882 Btu/kWh heat rate - the report discusses a means of more closely approaching the goal in this case.

EPRI PERSPECTIVE

PROJECT DESCRIPTION

One objective of the EPRI Fuel Cell Program is the development of an advanced fuel cell power plant capable of a < 7500 Btu/kWh heat rate (> 45% efficiency). Both molten carbonate and phosphoric acid fuel cell technologies are candidates for such a power plant. The primary determinants of power plant heat rate are a) the fuel cell performance (voltage) and b) the ability to thermally integrate subsystems and components into a power plant. This project is to establish component and subsystem definitions for two advanced fuel cell power plant types employing the molten carbonate technology. One type is a small (~5 MW), dispersed power plant using oil fuel; the other is a 675 MW, central station power plant using coal as the fuel. The focus of this project is to optimize the thermal integration in order to minimize the power plant heat rate. This interim report describes the definition of power plant configurations and establishes guidelines that will form the basis for the reference plant selection.

PROJECT OBJECTIVES

The general objective is to establish molten carbonate fuel cell power plant subsystem and component definitions that will achieve the targeted heat rate and meet other utility requirements inherent in the two applications. Specific objectives include:

- Defining overall plant performance, cost, and availability goals
- Developing reference power plant configurations
- Defining subsystems and component specifications
- Assessing the potential for the reference configurations to meet goals.

PROJECT RESULTS

The interim results reported herein describes:

- General design requirements for the two power plant types
- System analytic techniques and methodologies developed under the project
- Seven coal power plant and one oil power plant configurations.

Findings to date include:

- A coal-fueled configuration with a heat rate of 6785 Btu/kWh is identified; the best oil-fueled configuration identified to date has a 7882 Btu/kWh heat rate.
- A 6800 Btu/kWh heat rate is a realistic goal for a 675 MW coal-fueled power plant; a 7500 Btu/kWh heat rate is realistic for small oil-fueled plants.
- Oxygen-blown gasification results in better plant efficiency than air-blown.
- Carbon formation in the anode and sulfur buildup in the electrolyte must be avoided through power plant design consideration.

The efforts to date have provided an excellent foundation for understanding and optimizing molten carbonate power plants. The continuation of the project should result in the selection of reference designs, a preliminary costing of those designs, a preliminary costing of those designs as well as a determination of the sensitivity of the plants' cost and performance on the basis of such parameters as gasifier type, pressure, cooling concept, etc.

Arnold P. Fickett, Project Manager
Fossil Fuel and Advanced Systems Division

CONTENTS

ILLUSTRATIONS

TABLES

Section 1

EXECUTIVE SUMMARY

PROGRAM BACKGROUND

This Interim Report describes work conducted by the General Electric Company under EPRI contract RP 1085-1, "Molten Carbonate Fuel Cell Power Plant System Evaluation" over the period June, 1978 through December, 1978. The program's scope includes definition of fuel cell utility power plant design goals, definition and parametric evaluation of both coal-fired and oil-fired power plants, development of required system analysis tools, and derivation of fuel cell requirements which will enable the achievement of plant goals. Work is continuing to select reference oil and coal plant configurations, to establish cost information, and to define detailed fuel cell specifications.

The general objective of this "Molten Carbonate Fuel Cell Power Plant System Evaluation" Program is to establish requirements and goals for molten carbonate fuel cell development derived from utility generating plant applications. Two power plant types are under study, a small (5 MW) oil-fired plant for distributed generation and a large (675 MW) coal-fired central plant. Secondary objectives of the program include definition of system fuel cell trade-offs and sensitivities, development of necessary analysis methods, definition of fuel cell test data requirements, and identification of development needs and improvements for plant components, other than the fuel cell.

The general technical approach includes definition of overall plant performance, cost, and availability goals; definition and evaluation of major plant design options; selection of reference plant configurations for parametric sensitivity studies; and definition of sub-system specifications. We employ the same approach for both the coal-fired and oil-fired plants.

We adopted certain ground rules to place broad limits on the study's scope: Fuel specifications for both coal and oil plants, the assumption of the "Middletown" site, and the restriction of coal plant fuel supply evaluation to the Texaco entrained bed gasifier.

We began work on the program with a literature review of fuel-cell power plant concepts; next, we conducted a utility generation mix study to establish competitive cost and performance goals, summarized later in this report. A baseline study was then conducted. Representative, state-of-the-art plant cycle concepts were taken from the literature and critically compared with the plant performance goals, for adherence to known restraints and identification of key plant design parameters. This study's outcome led to the selection of candidate cycles from which one may, based on appropriate scoping studies, select a reference plant. This reference plant will then form the basis for future studies directed at its optimization.

Detailing the reference plant, both in terms of performance and cost, coupled with appropriate trade-off studies, permits development toward the optimum plant. One could then compare the plant goals with the predicted plant characteristics and define the subsystem characteristics. This evaluative process will indicate technology development needs and areas for further study in the plant system.

One may summarize the approach as follows:

1. Evaluate prior studies.
2. Establish plant goals and requirements.
3. Define and prepare necessary analysis techniques.
4. Establish plant evaluation guidelines through baseline studies.
5. Establish and evaluate cycle concepts.
6. Select reference plant for further study.
7. Establish trade-off parameters.
8. Expand detail of reference plant, including costs.
9. Conduct trade-offs.
10. Update reference plant and measure against goals and requirements.
11. Establish plant subsystem requirements (performance, cost and development).

SUMMARY OF FINDINGS

Our considerations of fuel-cell power plant integrated systems have led us to the following evaluations:

- An efficiency of 50% (6800 Btu/kWh heat rate) is a realistic goal for a large, 675 MW, coal-fired power plant utilizing fuel cells in an integrated system design. Cycles with this calculated efficiency are described.
- Oxygen-blown gasification in the coal-fired plant shows a plant efficiency improvement of approximately 3 points over air-blown, and substantially reduces gasification and cleanup equipment size.
- Reheat gas turbines improve coal-fired plant efficiency by 2 points, but at the cost of increased complexity.
- Carbon formation in the fuel cell anode is a key constraint of the plant design; use of anode recirculation may control it.
- The reduction in anode inlet fuel gas hydrogen concentration caused by anode gas recirculation indicates the need for laboratory testing on very lean gases.
- Anode gas recirculation may lead to sulfur build-up problems in the anode if sulfur is transported through the electrolyte. Anode venting and/or recirculation loop sulfur removal are possible solutions to this problem.
- The realistic efficiency goal of a small, 5 MW, dispersed oil-fired power plant is established as 45.5% (7500 Btu/kWh heat rate).
- We have identified a configuration for an oil-fired plant, which has a calculated efficiency of 43.3% (7882 Btu/kWh heat rate).
- The sooting tendency of the oil reforming equipment limits the oil-fired power plant efficiency.
- Hybrid reformers, currently under development, are shown to offer the promise for small dispersed oil-fired plants which exceed the stated efficiency goal of 45.5% (7500 Btu/kWh heat rate).

DESIGN REQUIREMENTS AND GOALS

The general design requirements and goals for the two power plant configurations are summarized in Tables 1-1 and 1-2. This Report presents a number of cycle arrangements which address the approaches to achieving the goals. In addition, it describes the system analysis techniques developed under the program. Future work will include selection of reference cycles, and parametric sensitivity evaluation with economics and preparation of subsystem specifications.

Table 1-1

GENERAL DESIGN REQUIREMENTS AND GOALS FOR A COAL-FIRED INTEGRATED FUEL CELL POWER PLANT

REQUIREMENT	
Central Station Power Plant	
Power Level	~675 MW(e)
Fuel	Illinois #6 Coal
Site Characteristics	"Middletown" Except for Cooling Tower Heat Rejection
Environmental	Projected 1985 Federal Requirements

GOALS		
1.	Base Load Duty with Daily* Load Following Capability	
2.	Heat Rate	6800 Btu/kWh
3.	Installed Capital Cost (1978)	$800 kW(e)
4.	Plant Availability	85%
5.	Life (75% Capacity Factor)	
	Fuel Cell Stacks	6 Years
	Balance of Plant	30 Years

*Large load changes response within two hours.
Small load changes response rate up to 2%/minute.

METHODOLOGY

Baseline plant cycles were established for both the coal-fired and oil-fired applications early in the study to focus the system performance evaluation activities. The baseline cycle configurations were directly derived from the published work of other contributors, tempered and modified following in-house subsystem evaluations. It was unnecessary for these baseline plants to represent optimum configurations, from either a performance or overall economic viewpoint. However, we attempted to have the baseline cycle selections reflect thinking which could allow definition of an optimum cycle by variation of the cycle arrangement.

Table 1-2

GENERAL DESIGN REQUIREMENTS AND GOALS
FOR THE OIL-FIRED POWER PLANT

REQUIREMENTS		
1.	Dispersed Station Plant (Industrial Application)	
2.	Power Level	4 - 5 MW(e)
3.	Fuel	No. 2 Fuel Oil
4.	Site Characteristics	"Middletown" Modified for Industrial Application
5.	Environmental	Projected 1985 Federal Requirements
GOALS		
1.	Intermediate Load Duty with Load Following Capability*	
2.	Heat Rate	7500 Btu/kWh
3.	Installed Capital Cost (1978)	$300/kW(e)
4.	Plant Availability	90%
5.	Life (50% Capacity Factor)	
	Fuel Cell Stacks	9 Years
	Balance of Plant	30 Years

*Able to load from 25% to 100% of nameplate MW and reverse, within 1 minute

Specific objectives of the baseline plant evaluations were:

1. To perform an independent performance assessment for comparison with the respective coal- and oil-fired plant performance goals;

2. To establish performance benchmarks for comparison with later evaluation of system parameters and subsystem options;

3. To quantify the influence of specific subsystem performance and operating limitations on overall plant efficiency and operation; and

4. To evaluate specific plant operating parameters and subsystem alternatives as the basis for selection of a reference plant configuration for further technical and economic evaluation.

As a result of these baseline studies we formulated important design guidelines which yielded for performance evaluation one oil- and seven coal-fired power plant cycles.

CYCLE DESIGN GUIDELINES

The guidelines summary follows below:

High Coal to Fuel Conversion Ratio

A high fuel source chemical energy conversion ratio (high fuel gas $CO+H_2$) is important because the fuel cell, which can electrochemically convert only the CO and H_2 fraction of the fuel gas makes the largest contribution to plant output. High oxidant blast temperature to the gasifier significantly enhances this ratio, but a high blast temperature such as 1500 ^{o}F can only be efficiently achieved through the use of a raw fuel gas to air regenerative heat exchanger. Such a device is considered developmental. The air-blown systems under consideration are therefore limited to those in which air preheat temperatures are achieved by the heat of compression.

High Fuel Cell Efficiency

Cycle configurations and operating conditions which maximize fuel cell efficiency are obviously desirable, and thus operation at high fuel utilization, such as 85%, is important. Anode recirculation is employed to introduce H_2O and CO_2 into the anode inlet gas to establish soot-free fuel gas compositions at some cost in cell efficiency. Peak cell efficiency is typically achieved at 50 to 75% excess air to the cathode in the studied cycles. However, the variation of voltage with excess air in the range of 75 to 200% is small, and other considerations such as gas turbine output and stack losses are involved in the selection of this parameter.

High Bottoming Cycle Power Conversion Efficiency

Some arrangement of gas and steam turbine generators must convert sensible energy of the fuel cell discharge stream. The most efficient arrangement is one where the entire heat content of the fuel cell discharge is delivered to a gas turbine, which then converts a portion of this heat to electricity and passes the balance

to a steam cycle and the exhaust stack. Heat delivered to the steam cycle is converted with an efficiency of 38%. If the same high-quality heat were first converted by the gas turbine expander at an efficiency of 90%, the remaining exhaust heat content could still be converted by the steam turbine.

High Steam Cycle Efficiency

High steam cycle efficiency is obviously important to the achievement of overall cycle efficiency. This implies the use of a high-pressure (2400 psi) reheat steam cycle. A 950 ^{o}F temperature is a reasonable compromise between peak efficiency (1000 ^{o}F) and concern for peak metal temperature in the high-temperature steam generator.

Integration of Oxidant Supply Compressors into the Power Conversion Cycle

A major parasitic power item with both oxygen- and air-blown gasifier systems is the oxidant supply compressor power. This power can be most efficiently supplied through utilization of a fuel gas expander turbine for compressor drive. This turbine operates on the pressure difference between gasifier cleanup and the fuel cell.

Minimization of Cleanup System Parasitic Power and Process Steam

The plant parasitic power typically amounts to 5% of the plant output, hence its minimization is important. It should be noted that the reduced clean-up system volume flow in an oxygen-blown gasifier cycle inplies a reduction in this parasitic power consumption.

COAL-FIRED PLANT STUDIES

We studied seven coal-fired power plant cycles with the following objectives:

1. To identify the advantages and disadvantages of oxygen- versus air-blown gasifier systems.
2. To formulate characteristics of high efficiency systems.
3. To identify alternative system flow circuits and the associated components.
4. To comparatively evaluate alternate cycle configurations and major parameter selections with respect to efficiency, degree of technical risk, and system and component complexity.
5. To identify a preliminary selection of the reference plant for further optimization and more detailed definition.

The plant shown in Figure 1-1 utilizes an oxygen-blown gasifier, Selexol cleanup system, and a partially cascaded bottoming cycle. To date, it is one of the more promising configurations identified for the coal-fired application.

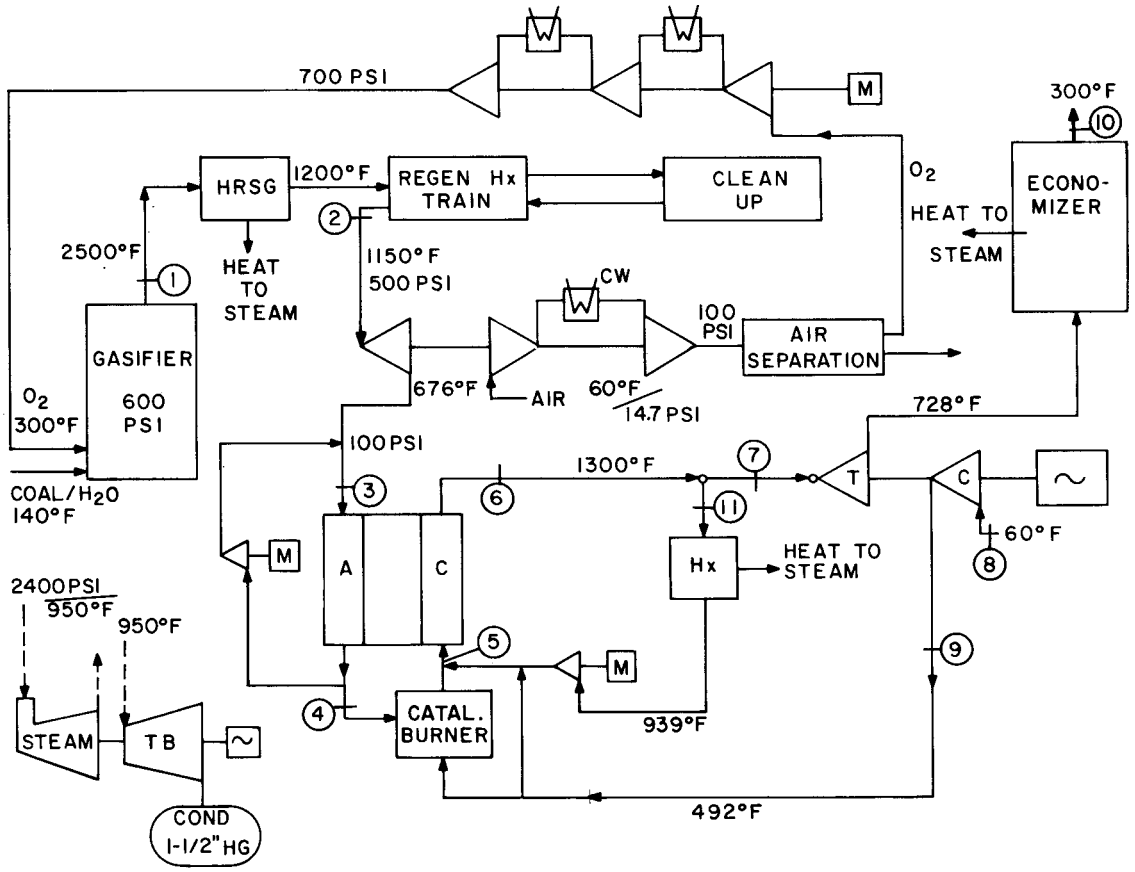

Figure 1-1. Oxygen-Blown System with Partially Cascaded Bottoming Cycle

This plant exhibits an efficiency of 50.3% (6785 Btu/kWh heat rate), and exceeds the program goal. The fuel cell supplies 67% of the plant output. The other six plant configurations, described in the text, follow with their computed efficiencies:

Case#	Figure#	Cycle	Cathode Excess Air	Plant Efficiency	Plant Heat Rate (Btu/kWh)
1	3-4	Oxygen-blown, partially cascaded bottoming cycle	100%	50.3%	6785
2	3-4	Oxygen-blown, partially cascaded bottoming cycle	20%	50.0%	6826
3	3-5	Oxygen-blown, fully cascaded bottoming cycle	190%	51.7%	6602

4	3-6	Oxygen-blown, regenerative gas turbine	90%	46.6%	7324
5	3-7	Air-blown, fully cascaded, booster intercooler	76%	45.8%	7452
6	3-7	Air-blown, fully cascaded, no booster intercooler	109%	49.1%	6951
7	3-8	Air-blown, simple gas turbine, no booster intercooler	50%	46.9%	7277

In general, we found that the gross outputs of air- and oxygen-blown systems were similar, but that the increased parasitic power consumption caused by the air-blown system's greater flow rates created 2-3% efficiency loss. The use of a reheat gas turbine to achieve full cascading in the bottoming cycle generated up to a 2% advantage in plant efficiency.

We found it possible to configure all plants so that the fuel entering the fuel cell anode would equilibrate to a soot-free composition.

OIL-FIRED POWER PLANT STUDY

An oil-fired power plant cycle was established to address small, distributed installations where minimum capital cost, prompt response characteristics, and minimum environmental intrusion were the paramount considerations. The plant cycle is a straightforward arrangement of an autothermal reformer and a zinc oxide sulfur scrubber with periodic off-site disposal of sorbent media, followed by the molten carbonate fuel cell/inverter subsystem. The requirements of minimum capital cost and small size have eliminated consideration of waste heat bottoming cycles. Consequently, the distributed oil-fired power plant provides a significant amount of excess sensible heat, beyond that which the autothermal reformer can utilize. This heat energy could be made available to a local consumer for space or process heating. In quoting power plant performance, this "co-generation" heat receives no credit.

The plant performance was analyzed with comprehensive analytical models evaluating the autothermal reformer and the fuel cell. A consistent set of fuel-cell operating parameters and sizing criteria were employed for all cycles investigated, allowing specific fuel cell voltage and power density to accurately reflect the anode and cathode gas compositions. Overall efficiency of the oil-fired plant was a predicted 43.3% (7882 Btu/kWh heat rate), relative to the study goal of 45.5%

(7500 Btu/kWh heat rate). Evaluation of the sensitivity of plant efficiency to component variation isolated autothermal reformer improvements as the key approach to achieving the performance goal. An increase in the reformer conversion efficiency, defined as the heating value of the fuel gas (H_2+CO) content divided by the heating value of the oil, directly increases the amount of chemical energy available to the fuel cell and improves the fuel cell's efficiency via an increase in specific heating value. The precipitation of solid carbon at a minimum value of air/carbon ratio, determined from experimental work, currently limits the degree to which system excess sensible heat replaces combustion within the reformer.

The current oil-to-fuel gas heating value conversion efficiency is in the range 0.98 - 0.99. Systems evaluation of the reformer coupled to the fuel cell indicates that a conversion efficiency of approximately 1.04 is necessary to achieve the performance goal. Some relaxation of this conversion efficiency is possible through increased cell voltage and/or optimum arrangement of the fuel-cell heat rejection. The work performed to date specifically excluded capital cost as a figure of merit and, additionally, concentrated on the most influential variables.

Future efforts will select the reference power plant configurations, develop cost information, and define appropriate areas for continued attention.

Section 2

THE FUEL CELL IN A UTILITY POWER PLANT

INTRODUCTION

The molten carbonate fuel cell is an energy conversion device which offers the potential for high efficiency, ease of integration into power plant cycles, and compatibility with fossil fuel sources. This section discusses the assumptions related to the fuel cell used in this study. Additionally, it offers some limitations and operational considerations.

The thrust of this integrated fuel cell power plant system study, to date, is toward the definition of reference cycles for the coal- and the oil-fired plants, on which the subsequent detailing and trade-offs may be based. To simplify this process and to reflect the available test data, we have used a single fuel cell design for all the work to this point. While this design has, of course, reacted differently to the differing gas streams in the various studies, key assumptions such as maximum utilization, current density and losses remain constant. Activities planned later in the course of this work explore the various impacts of some of these assumptions.

FUEL CELL STUDY ASSUMPTIONS

Several extremely important fuel-cell parameters are involved in a detailed analysis of a power plant system. However, rigorous treatment of all these issues at this stage of the study would prevent the identification of trends, guidelines, and the inherent features of the systems being evolved. For this reason, we judged it prudent to select a unifying set of assumptions for the fuel cell, for all of the cycle options being considered. It will be appropriate to evaluate the impact and validity of these assumptions later.

In this section we state those assumptions and, where appropriate, indicate the reason for their selection. Note that most of this information appears elsewhere in this report; this section serves as a single reference location.

Current Density

The ECAS study (1) identified 161.5 mA/cm^2 (150 amp/ft^2) as an achievable development goal for operating current density. That same study indicated that this current density may be in the vicinity of the economic optimum. While present testing indicates that the goal may indeed be achievable, establishment of current density remains an objective of this study. Meanwhile, we adopted the figure of 161.5 mA/cm^2, pending later study.

It is to be noted that for the fuel gases being studied in these electric utility power plants, peak power density occurs at about 600 mA/cm^2 and peak efficiency at 0 mA/cm^2. While the former operating condition may never be realizable this comparison does indicate the wide latitude in this parametric selection.

Utilization

As discussed earlier, the fuel cell is the highest efficiency energy conversion device in the power plant, and thermodynamically lies at the "top" of the cycle. Thus, an initial assumption is that the selected utilization will be as high as possible, in order to maximize the energy converted at this favorable efficiency.

For several reasons, 100% utilization is not possible and current testing has already proved the feasibility of utilization in excess of 80%.

For the purposes of this study, we have selected an overall utilization of 85%.

Carbon Formation

To ensure a consistent approach to the carbon formation problem, we assumed that the conditions (presumably equilibrium) at the fuel-cell anode (inlet in particular) will determine carbon formation.

This assumption yields a consistent study approach, and, of course, is simpler to assess than consideration of reaction kinetics. However, one should note, particularly in the area of the first contact with the electrode's catalytic action, that an important assumption is thus implied about kinetics. Specifically, when the gas moves from its prior condition to the equilibrated condition, the rate of the water gas shift reaction is faster than any carbon formation reaction.

Methane Formation

The uncertain and available data on the formation and reformation of methane in the fuel cell anode, makes a definitive statement impossible. However, based on a judgment of the relative test procedures, we have assumed that no methane forms in the fuel cell anode at this time.

Continuous monitoring of the available test data will permit re-evaluation of this assumption if appropriate.

A check is being made on plant performance impact, if the assumption is incorrect. In this impact evaluation, we assumed that the methane formation equilibrates irreversibly at the anode inlet.

Polarization Losses

Section 5, under the headline Fuel Cell Analytical Model Performance Evaluation, discusses studies conducted to validate the Fuel Cell Analytic Model. That discussion states that, based on the ECAS study (1), total polarization loss is linear with current density (for constant utilization) and has a value of 0.7 Ωcm^2. This is stated as an achievable goal by 1990. We also assumed that activation polarization losses are negligible.

An important remaining issue is the examination of this assumption when gas concentrations are very low. While such examination is outside the scope of this study, this question may be found to be an appropriate test recommendation.

Temperature

We have assumed, that the following temperatures exist in the fuel cell:

- Electrochemical reaction temperature (Used in Nernst voltage calculations) - 1250 ^{o}F.
- Anode gas exit temperature - 1300 ^{o}F.
- Cathode gas exit temperature - 1300 ^{o}F.
- Minimum gas inlet temperatures - 1000 ^{o}F.

OPERATIONAL CONSIDERATIONS

At this time, it is not within the scope of this study to evaluate plant operation in detail because the study is plant design oriented. Nevertheless, during the

course of our study, several important operational issues became evident. They follow below with little comment, but they deserve future attention.

Fuel Cell ΔP	Current cell development activity centers around cells with low (few psi) electrode to electrode pressure capability. With the high flow rates encountered in these cycles, and the complex manifolding implied, it is highly improbable that maintenance of these low ΔP values will be possible. During transient conditions, with the extensive piping and pressure vessels, it will be difficult to regulate ΔP that closely.
Power Control	The power inverter technology available today makes selection of many power control modes very easy. Thus, as the load or gas compositions change, the fuel cells can be maintained at constant voltage, constant current, or a combination of the two to give, for example, constant utilization. However, for mode selection one must consider not only the fuel cell but the downstream bottoming cycles. It is conceivable that inappropriate control modes will totally negate the inherent, high part load efficiency of the fuel cell by inadequate part load use of the bottoming cycles.
Thermal Control	The operating fuel cells' temperature range is somewhat narrow in comparison with other power plant machinery. This difficulty is compounded by the need for thermal control through operating condition selection, and there is also some question of the tile durability in thermal cycles. While this area is closely related to that of Power Control, one must pay very careful attention to this specific area before commitment to a given cycle and operating mode.

REFERENCES

1. "Integrated Coal Gasifier/Molten Carbonate Fuel Cell Power Plant Conceptual Design and Implementation Assessment." Energy Conversion Alternatives Study (ECAS), United Technologies Phase II Final Report, Report No. FCR-0237.

Section 3

COAL-FIRED POWER PLANT

INTRODUCTION

Section 3 describes activities directed at the selection of a reference plant cycle. The selected cycle will be the basis for future parametric evaluation and costing, and will improve by means of suitable trade-off studies. The selected plant must, at least, meet all the known component constraints, and attain as many design goals as possible prior to the commencement of such studies; this ensures a solid base for the ensuing cycle development efforts.

Initially, we conducted baseline evaluations, summarized in this section. Our objective was to develop background and useful study guidelines for a plant of this complexity.

Basic thermodynamic considerations dictated a 'cascaded' approach in which the fuel cell, a gas turbine and, finally, a steam cycle successively convert the energy flow. However, the selection of the cascading degree, the machinery, and the interface conditions for each conversion means, are the challenge in the plant design.

This section outlines plant requirements and the established goals for the coal plant. Further, it summarizes the results of baseline studies in which cycle design guidelines and analysis techniques were developed. These guidelines are then expanded in a discussion of current scoping studies, and of cycles conceived as candidates for the selection of the study reference cycle.

POWER PLANT REQUIREMENTS AND GOALS

Preliminary goals and requirements for the coal-fired plant have been outlined to provide a framework within which the system evaluations described in subsequent sections are performed.

Table 3-1 summarizes the general design requirements and goals for the coal-fired power plant.

Table 3-1

GENERAL DESIGN REQUIREMENT AND GOALS FOR A COAL-FIRED INTEGRATED FUEL CELL POWER PLANT

Requirements

1.	Central Station Power Plant	
2.	Power Level	675 MW(e)
3.	Fuel	Illinois #6 Coal
4.	Site Characteristics	"Middletown" Except for Cooling Tower Heat Rejection
5.	Environmental	Projected 1985 Federal Requirements

Goals

1.	Base Load Duty with Daily* Load Following Capability	
2.	Heat Rate	6800 Btu/kWh
3.	Installed Capital Cost (1978)	$800/kW(e)
4.	Plant Availability	85%
5.	Life (75% Capacity Factor)	
	Fuel Cell Stacks	6 Years
	Balance of Plant	30 Years

*Large load changes within 2 hours
Small load changes at a rate of 2%/minute

The specified fuel is Illinois #6 coal, representative of the highly-caking Eastern Bituminous coals which the plant will handle. Table 3-2 gives the composition of Illinois #6.

Table 3-2

COMPOSITION OF ILLINOIS #6 COAL

Proximate Analysis (Wt. %)

Moisture	4.2
Volatile Matter	34.2
Fixed Carbon	52.0
Ash	9.6
	100.0

Ultimate Analysis - DAF (Wt. %)

Carbon	77.26
Hydrogen	5.92
Oxygen	11.14
Nitrogen	1.39
Sulfur	4.29
	100.00
Higher Heating Value (HHV)	12,235 Btu/lb (as received)
Lower Heating Value (LHV)	11,709 Btu/lb (as received)

Regulations have not established definitive environmental standards for the construction and operation of a coal-fired fuel cell power plant. Lacking specific emission standards, the typical practice is to extrapolate standards for equipment that the plant might displace. Table 3-3 gives the existing environmental limits applicable to a new or modified large coal-fired combustion facility. Further, Table 3-3 also compares these limits with those projected to 1985 by General Electric and others. These projected standards are the design basis for the reference coal-fired power plant.

A heat rate goal of 6800 Btu/kW(e) ac, corresponding to a plant efficiency of 50.2%, has been established. This efficiency, coupled with an installed capital cost goal of $800/kW(e) ac (1978) and an availability of 85%, will compare favorably with other advanced central coal-fired power plants installed at the same time.

Table 3-3

CURRENT AND PROJECTED EMISSION STANDARDS
FOR THE COAL-FIRED PLANT

Pollutant	Current Standards	Projected 1985 Federal Requirements
SO_x	1.2 lb/10^6 Btu	90% Removal (0.7 lb/10^6 Btu)
NO_x	0.7 lb/10^6 Btu	0.6 lb/10^6 Btu
TSP	0.1 lb/10^6 Btu	0.03 lb/10^6 Btu

COMPONENT AND CYCLE CONFIGURATION CHARACTERISTICS FOR HIGH EFFICIENCY PLANT DESIGN

Preliminary studies were conducted using system concepts selected from a review of relevant, published work and from in-house subsystem evaluations. The studies' results established a benchmark to compare with other cycle concepts and subsystem options, and the techniques to conduct such evaluations.

The specific objectives of these preliminary studies were:

- Independent performance assessment of the selected cycle for comparison with performance goals.
- Identification of component constraints and their impact on plant performance and configuration.
- Establishment of criteria by which the interaction of the subsystems can be quantified.
- Identification of the key design parameters influencing plant performance.
- Establishment of candidate cycles from which a reference plant cycle can be selected for future study.

Based on these studies we have developed a set of guidelines and considerations for high efficiency coal-fired power plant design, a summary of which follows.

High Coal to Fuel Conversion Ratio

The coal to fuel conversion ratio is defined as follows:

$$\text{Conversion Ratio} = \frac{\text{HHV of } (H_2+CO) \text{ in Fuel Gas}}{\text{HHV of Raw Coal}}$$

where HHV = Higher heating value

A high fuel source chemical energy conversion ratio is important because the largest contribution to plant output is made by the fuel cell (67%) which can electrochemically convert only the CO and H_2 in the fuel gas and cannot convert sensible heat. The Texaco entrained bed gasifier specified for this program is compatible with either air or oxygen blowing and produces a product gas HV content essentially limited to CO and H_2 (very low methane). Reference (1) indicates that for the oxygen-blown Texaco gasifier the ratio of hydrogen and carbon monoxide heating value to input coal heating value is approximately 77%. Information received by General Electric from Texaco (2) indicates the relationship between the above fuel conversion ratio and blast air preheat temperature shown in Figure 3-1. As blast temperature increases, so does gasifier efficiency.

A high blast air temperature, however, such as 1500 ^{o}F, can only be efficiently achieved through the use of a raw fuel-gas to air, regenerative heat exchanger. Such a device is fraught with safety hazards and metallurgical risk. For this reason the air-blown systems considered herein have been limited in air preheat temperature level to that realizable by heat of compression; i.e., no heat is added to the gas beyond the gasifier boost compressor. This temperature has been limited to that realized in developmental aircraft compressors (1200 ^{o}F).

The oxygen-blown system, of course, does not suffer the penalty of having to heat the inert nitrogen through to gasifier discharge temperature, and thus the oxygen-blown system is somewhat less sensitive to lower oxidant blast temperature.

High Fuel Cell Efficiency

The fuel cell component electrochemically converts to electricity between 40% and 50% of the H_2+CO heating value content in the anode inlet gas, and at the same time

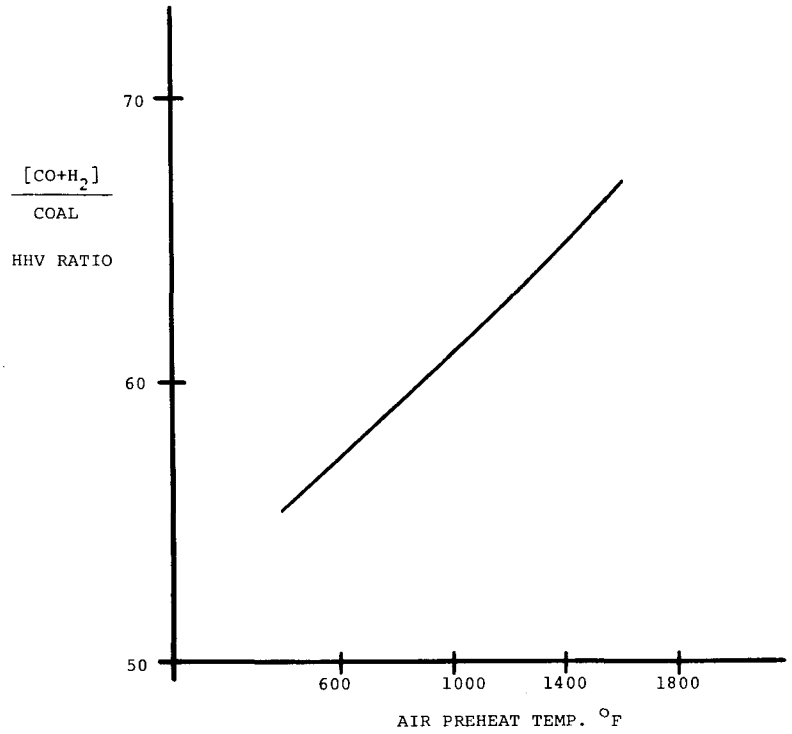

Figure 3-1. Texaco Gasifier Fuel Conversion Ratio versus Air Preheat Temperature

raises the temperature of the final product gases. These gases incorporate partially reacted air and oxidant supplied from a gas turbine and are at a level of 1200 to 1300 ^{o}F, which is suitable for gas turbine/steam turbine bottoming cycle power conversion. Since bottoming cycle power conversion at this temperature is less efficient than electrochemical conversion it is important to maximize the fuel cell efficiency. Operation capability at high fuel utilization, such as the 85% assumed in the present studies, is important. We have also assumed a relatively modest current density level of 160 mA/cm^2.

Carbon-free anode conditions require modification of the fuel gas. An effective method is to recirculate the anode exit gases to introduce H_2O and CO_2. However, one should note that this process degrades cell efficiency. Thus, for our design approach we chose to recirculate the minimum amount of anode gases necessary to achieve carbon-free anode conditions. System temperatures preclude any effective cooling on this recirculation loop, and thus we achieved cell cooling through additional recirculation on the cathode side via a heat exchanger.

Further consideration of anode recirculation leads to three interesting observations:

a). Anode recirculation reduces the possibility of carbon formation but causes reduction of the anode inlet concentration. The question raised then is whether or not it is practical to operate the fuel cell at the assumed utilization and current density. Furthermore, the impact on the polarization loss currently assumed to be 0.7 cm^2 needs assessment.

b). There is postulated the existence of a 'sulfur pump' effect in the fuel cell. Specifically, the sulfur in the fuel passes through the anode, into the catalytic burner, and then to the cathode. Electrochemical action may capture the sulfur in the electrolyte and transport it back to the anode. This mechanism would cause a concentrated sulfur buildup in the cell.

The use of anode recirculation does offer a mechanism by which one may 'flush' the anode of sulfur and prevent its buildup. Figure 3-2 shows a scheme in which a scrubber is used to reduce the sulfur concentration in the recirculation path.

Use of a 50% efficient sulfur scrubber in a system with a 50% recirculation flow would hold the sulfur level to twice the incoming level, assuming that none flows from the cathode exit. This is contrasted with an unbounded buildup with no such scheme.

c). The third observation relates to methane formation. There is some evidence, unsubstantiated as yet, that indicates methane may form in the fuel cell anode. If this is so, serious fuel cell performance penalties will result through the unproductive capture of hydrogren and carbon monoxide. We found that anode recirculation was a powerful tool in suppressing this formation on an equilibrium study basis, as is the reduction of fuel cell pressure.

Another parameter affecting fuel cell efficiency is excess air. Peak efficiency is achieved at 50 to 75% excess air in the cases studied. However, the variation of voltage with excess air in the range 50 - 200% is small, and other cycle considerations such as gas turbine output and feedwater heating duty must be involved in the selection of this parameter.

High Bottoming Cycle Power Conversion Efficiency

Some arrangement of gas and steam turbine generators must convert sensible energy of the fuel cell discharge stream. The most efficient arrangement is one where the entire fuel cell discharge heat content is delivered to a gas turbine, which converts a portion of this heat to electricity and then passes the balance to a steam cycle and the exhaust stack. The turbine discharge gas is passed to a steam generator/economizer before going to the exhaust stack at a temperature of 300 ^{o}F or less.

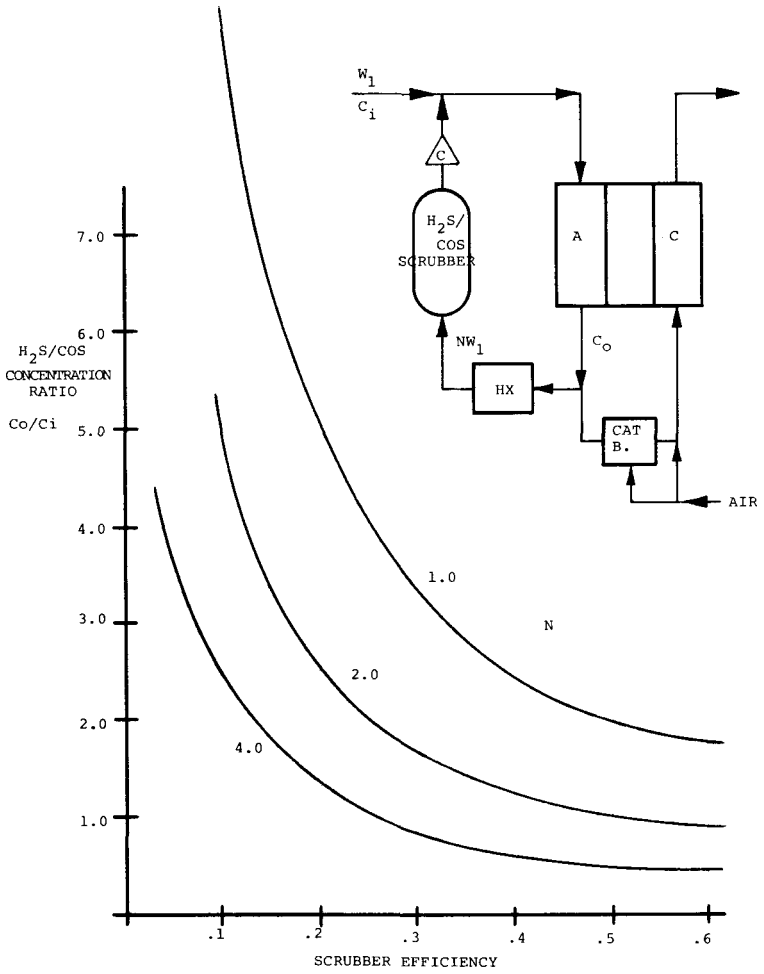

Figure 3-2. H_2S/COS Scrubber in Anode RC Path

Heat delivered to the steam is converted at the steam cycle efficiency whereas the high-quality heat converted by the gas turbine expander is converted at an efficiency of 90%, the only losses being electrical, and miscellaneous mechanical and heat losses not returned to the gas stream. In such a cycle one must exercise care to ensure that the amount of heat cascaded to the steam from the gas turbine exhaust does not exceed the requirements of the non-extraction steam cycle for heat at the relatively low temperature level of the exhaust gas, and that the ratio of feedwater flow to gas flow is compatible with an economizer heat transfer process providing an acceptable exhaust stack temperature (300 ^{o}F or below). As the exhaust stack temperature rises so do the exhaust stack losses, thus reducing the heat delivered to the steam.

We have identified and considered three bottoming cycle configurations which achieve the cascaded condition described above. Only one of these, however, provides cascaded heat in an amount and at a temperature level compatible with a high-pressure reheat steam cycle.

This most efficient configuration is a fully cascaded configuration employing a reheat gas turbine. Here the cathode discharge gas is divided into two streams, one going directly to the high-pressure turbine and the other to a heat exchanger which reheats the high-pressure turbine discharge before it goes to the low-pressure turbine. From the reheater outlet this gas stream is recycled to the cathode inlet, thus heating the cathode inlet flow. Because of the relatively low-pressure ratio of the low-pressure turbine, and because of the reheat at the low-pressure turbine inlet, the exhaust temperature is sufficiently high for effective feedwater heating and partial vaporization of 2400 psi steam. Furthermore, the ratio of feedwater flow to stack gas flow is adequate for maintenance of a satisfactory stack temperature. Because this cycle accomplishes effective cascading of energy through a gas turbine to a high-pressure reheat steam cycle, it achieves better efficiency than the alternates. With all of the fully cascaded cycles, the gas turbine air flow is fixed by other cycle parameters and thus is not subject to independent selection.

As an alternative to a fully cascaded bottoming cycle one may employ a partially cascaded configuration at a modest sacrifice of efficiency from the reheat turbine cycle. Thus, one may avoid the complications of a reheat gas turbine and the necessity for development of a turbine of this type.

In the partially cascaded bottoming cycle the cathode discharge flow is divided, one stream going to a steam generator heat exchanger, and then returning to the cathode inlet. With this cycle the gas turbine air flow can be selected as an optimum compromise between gas turbine output, feedwater to exhaust gas flow ratio, and fuel cell efficiency. The partially cascaded cycle optimizes at a lower pressure ratio than the reheat turbine cycle.

High Steam Cycle Efficiency

High steam cycle efficiency is obviously important to the achievement of high overall cycle efficiency. This implies the use of high pressure (2400 psi) reheat steam cycle with a 950 ^{o}F steam temperature. At 1-1/2 Hg condensing pressure this steam cycle, without extraction heating of feedwater, has an efficiency of 38%.

Integration of Oxidant Supply Compressors into the Power Conversion Cycle

A major parasitic power item with both oxygen- and air-blown gasifier systems is the oxidant supply compressor power. This power can be most efficiently supplied through utilization of a fuel gas expander turbine for compressor drive. This turbine operates on the pressure difference between gasifier cleanup and the fuel cell. In the oxygen-blown systems, compressor intercooling can effectively improve efficiency by reduction in compressor power. In the air-blown systems, intercooling is not effective since it reduces blast temperature. High efficiency (utility/aircraft gas turbine state of the art) turbo-machinery should be employed for oxidant supply as well as for power conversion.

Minimization of Cleanup System Parasitic Power and Process Steam

The fuel gas cleanup system requires a significant amount of parasitic power, most of which is refrigeration and pumping power for Selexol absorbent liquid. Power requirements for an oxygen system are estimated to be approximately 6% of the coal HHV, as compared to about 1.2% for an air oxidant system. This difference reflects the smaller number of fuel gas moles per pound of coal and the smaller flow rate of absorbent which results from lower gas flow rate, higher partial pressure, and increased solubility of the acid gas components which dissolve in the absorbent. This is an important advantage for the oxygen system.

REFERENCE COAL-FIRED PLANT CYCLE DEVELOPMENT

The current thrust of activities is toward the selection of a reference plant cycle upon which further studies may be confidently based. To this goal, we conducted studies in which the design principles and considerations discussed in the foregoing were applied to develop, analyze, and compare candidate cycles from which the reference cycle may eventually be selected.

This section describes the objectives, the analytical procedures, the cycles considered, and the study results.

Cycle Study Objectives

The objectives of the alternate cycle studies included the following:

1. To identify the advantages and disadvantages of oxygen- versus air-blown gasifier systems.

2. To formulate characteristics of high efficiency systems.

3. To identify alternative system flow circuits and the associated components.

4. To comparatively evaluate alternative cycle configurations and major parameter selections with respect to efficiency, degree of technical risk, and system and component complexity.

5. To identify a preliminary selection of the reference plant for further optimization and more detailed definition.

Cycle Study Assumptions

We conducted the study on the basis of the following assumptions:

1. Gasifier Performance/Coal Specification

   The coal-fired Texaco oxygen-blown gasifier performance (coal/water slurry, oxygen inputs, product gas composition, temperature and pressure) as defined in Reference (1) is assumed. Illinois #6 coal as specified in Table 3-2 is assumed. Performance of an air-blown version of the Texaco gasifier for blast air temperatures of 600 ^{o}F and 1500 ^{o}F is based on data supplied by Texaco (2). An interpolation of gas composition, and coal to H_2+CO heating value ratio has been performed to estimate performance at 1250 ^{o}F blast temperature, using the model described in AIR-BLOWN GASIFIER (TEXACO) MODEL.

2. Steam Generator for Cooling of Gasifier Effluent Gas

   It has been assumed that a steam generator heated by a direct pass of gasifier product gas can be developed for application to a 2400 psi/950 ^{o}F/950 ^{o}F reheat steam cycle. The high temperature steam generator in the preferred cycle completes feedwater heating and initiates vaporization. In an alternate cycle final superheat and reheat are required. Fuel gas is assumed to leave the steam generator at a temperature of 1200 ^{o}F.

3. Fuel Gas Temperature Steam Generator Outlet

   The fuel gas is cooled to a temperature below 100 ^{o}F for cleanup by passage through a regenerative heat exchanger train, which also reheats the cleanup gas to a temperature of 1150 ^{o}F. A large portion of the water and some of the CO_2 are assumed to be removed by the cleanup process, along with essentially all of the H_2S, COS, and NH_3. To expedite scoping study calculations for the oxygen- and for the air-blown cases, the argon and methane are ignored. Potential formation of carbon and methane in the fuel gas in the pre-fuel cell processing is recognized but not considered in the scoping study calculations.

4. Carbon and Methane Formation in the Fuel Cell

   Fuel cell pressure level selection and anode recirculation are employed to prevent the formation of carbon in the fuel cell, in

accordance with a computerized gas equilibrium calculation. In most cases these calculations indicate the formation of a small amount of methane. This has been ignored in the scoping study calculations. However, the effect of this methane on the performance of one of the cases has been estimated.

5. Parasitic Power Estimates

Compressors for oxidant supply and the expanders to drive them are assumed to have efficiency levels representative of high performance utility and aircraft gas turbine equipment. Integration of the oxidant supply system into the cycle so as to extract energy from the pressure let down between the clean-up system and the fuel cell is assumed. This work recovery has been credited in arriving at estimates of net parasitic power for oxidant supply. Additional parasitic power for the plants employing oxygen-blown gasifiers has been estimated at 2-1/2% of the coal HHV (approximately 5% of the plant gross electrical output). For the air-blown gasifier plants, 3% of the coal HHV is assumed because of higher cleanup system parasitic power.

6. Cycle/Fuel Cell Parameter Selections

Gasifier pressure has been fixed at 600 psi for all cycles. Fuel cell pressure has been selected at estimated close-to-optimum levels for individual cycles. The fuel cell temperature has been selected at 1300 ^{o}F for all cycles. Fuel utilization and current density levels have been selected at .85 and 160 mA/cm^{2} respectively.

Cycle Study Analytical Procedure

We performed the Preliminary Comparative Performance Calculations for the alternate air and oxygen plants and developed the following procedure:

1. Using the gasifier coal feed rate, product gas flow rate, composition data, and the product gas temperature, we determined from tables (3) the heat delivered to steam in the high-temperature steam generator when the gases cool to 1200 ^{o}F. All mass and energy quantities are handled on a 1 pound of coal basis. Gasifier pressure is 600 psia.

2. Next, we determined the fuel gas mass per pound of coal and the composition at the clean gas discharge of the regenerative heat exchange train. We assumed a temperature/pressure level of 1150 ^{o}F/500 psi at this station. Further, we assumed that the cleanup process removed all H_2S, COS, and NH_3, and ignored small traces of Ar and CH_4. In the case of oxygen-blown plants, we ignored N_2.

3. Then we calculated the expansion process of the clean gas through a turbine from a pressure level of 500 psi to the fuel cell pressure, and determined the gas temperature at the turbine discharge.

4. We carried out an overall fuel cell subsystem heat balance as shown in Figure 3-3.

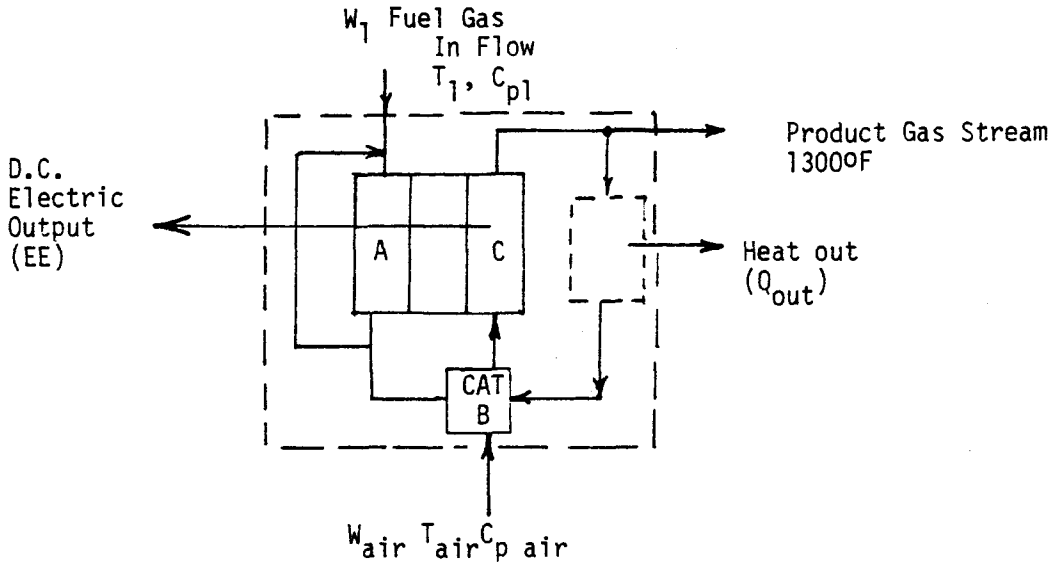

Figure 3-3. Fuel Cell System Energy Balance

Enthalpy in fuel gas + Enthalpy in air stream
= Enthalpy in Products + Heat Out (Q_{out})
- Electrical Output (EE)

5. We calculated gas composition changes occurring in the anode, using an assigned value of fuel utilization. We determined the anode outlet gas composition under shift reaction equilibrium condition. Iterating if necessary, we determined amount of anode recirculation required to establish a carbon-free equilibrium mixture at the anode inlet. (The General Electric equilibrium computer program is used in this process.) Also, we determined that the equilibrium mixture has a minimum temperature of 1000 °F or more, increasing recirculated flow if necessary to meet this condition.

6. Using the selected value of fuel utilization, the heat of reaction of the total fuel supplied, and an estimated value of dc output, we determined the total required fuel cell cooling enthalpy change; we estimated cooling on anode side from fuel inlet flow, Cp, and difference between fuel cell temperature and fuel gas inlet temperature. Then we calculated cathode cooling as a total cooling minus anode cooling. From cathode cooling and an assigned value of cathode inlet temperature, we determined cathode recirculation flow for cases where this is involved. Where no recirculation is involved we calculated cathode inlet temperature from cathode cooling heat balance. We calculated cathode burner heat balance as a check on the results of cathode cooling heat balance. We verified satisfactory heat transfer conditions in recirculating loop heat exchangers if these existed, and reselected cathode inlet temperature if necessary.

7. Based on the anode gas compositions and determined values of W_{Air} and W_{RC} (in cases where W_{RC} exists), we determined cathode inlet gas composition.

8. Based on gas compositions at anode inlet, anode outlet, cathode inlet, and cathode outlet, we determined zero polarization voltages using the Nernst equation for anode inlet/cathode outlet and anode outlet/cathode inlet (counterflow). We determined log mean of these voltages and applied a polarization correction based on an assumed overall polarization resistivity of .7 Ωcm^2 and a mean current density of 160 mA/cm^2.

9. We calculated the gas turbine output based on 1300 ^{o}F inlet temperature, 1250 ^{o}F reheat temperature (for the RH tb case) and 60 ^{o}F compressor inlet temperature. Gas flow rate and composition will be determined from fuel gas anode inlet flow (ahead of mixing) and from the air flow.

10. We calculated the total heat input to the steam cycle based on:

    - Input to raw gas cooler.
    - Input to the cathode recirculation loop heat exchanger (if used).
    - Input to economizer.

    The economizer heat input is calculated from the turbine gas flow, ΔT between turbine discharge and the assumed stack temperature of 300 ^{o}F. A check on the feedwater heating heat transfer may dictate a higher stack temperature. We determined gross electrical output based on the sum of the fuel cell ac output, gas turbine generator output, and steam turbine output, using a steam turbine generator efficiency of 38% (2400 psi/ 950 ^{o}F/950 ^{o}F with 1.5" Hg) and subtracted parasitic power from gross output to determine net output (plant efficiency).

Note that steps 4, 5, 6, 7, and 8 are mechanized by use of the fuel cell model described in Section 5.

Discussion of Scoping Study of Alternate Cycles

Figures 3-4 through 3-8 illustrate the seven molten carbonate fuel cell power plants evaluated in the reference plant scoping study. The seven cases are described below. Flow data sheets are included as Tables 3-4 through 3-10. Table 3-11 compares the performance of the seven cycles.

The cases considered are:

Case#	Figure#	Cycle	
1	3-4	Oxygen-blown, partially cascaded bottoming cycle	- 100% Excess Air
2	3-4	Oxygen-blown, partially cascaded bottoming cycle	- 20% Excess Air
3	3-5	Oxygen-blown, fully cascaded bottoming cycle	- 190% Excess Air
4	3-6	Oxygen-blown, regenerative	- 590% Excess Air
5	3-7	Air-blown, fully cascaded. booster intercooler	- 76% Excess Air
6	3-7	Air-blown, fully cascaded, no booster intercooler	- 109% Excess Air
7	3-8	Air-blown, simple gas turbine, no booster intercooler	- 50% Excess Air

Oxygen-Blown System with Partially Cascaded Bottoming Cycle

Case 1. The fuel source for this system (Figure 3-4) is an oxygen-blown Texaco gasifier fed with a coal/water slurry at 140 ^{o}F and oxygen at 300 ^{o}F, 700 psi. The oxygen to coal ratio = .84 and the water to coal ratio = .44. Product gas temperature is 2500 ^{o}F. The gasifier pressure is 600 psi. The raw gas flow rate is 2.18 #/# coal. Gasifier effluent passes through the high temperature steam generator which incorporates an initial radiant section followed by a convection section. Slag and particulates are removed through lock hoppers. Steam generation duty includes completion of feedwater heating and partial vaporization. Gas temperature at the end of the Heat Recovery Steam Generator (HRSG) is 1200 ^{o}F. From the steam generator the raw fuel gas passes through the regenerative heat exchanger train where it cools to approximately 100 ^{o}F and water vapor condenses. The cleanup system is a Selexol physical absorption system including a COS converter, NH_3 scrubber, both gas and absorbent refrigeration units, an H_2S absorber and a steam stripper regenerator. The absorber operates at approximately 560 psi, 40 ^{o}F, and the regenerator operates at approximately 25 psi, 220 ^{o}F. A hydraulic pump-turbine unit conserves pumping power in the absorbent liquid flow circuit. The regenerator requires approximately .3 pounds of 50 psi steam per pound of coal, which it extracts from the steam turbine.

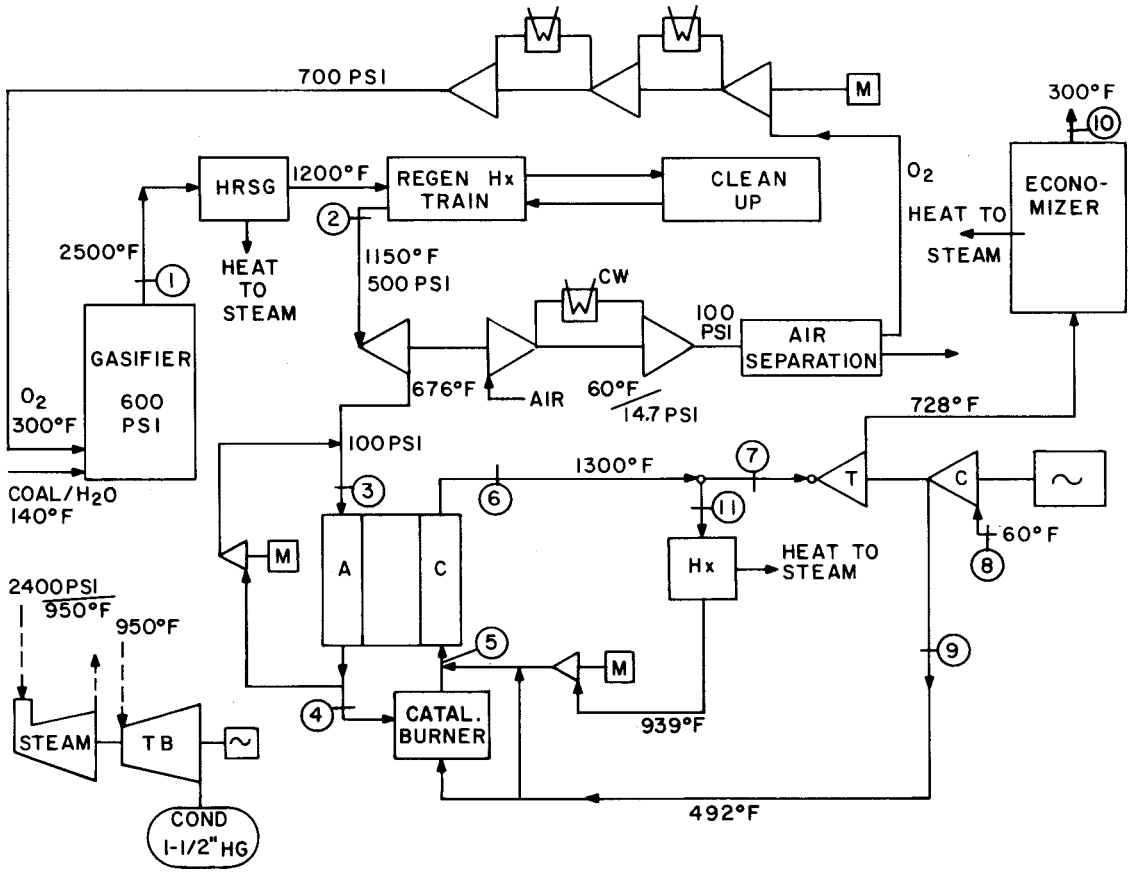

Figure 3-4. Oxygen-Blown System with Partially Cascaded Bottoming Cycle

The clean fuel gas flow leaves the Selexol system at approximately 75 ^{o}F and passes back through the regenerative heat exchanger train, leaving at 1150 ^{o}F. The flow rate of clean gas, after substantial water removal, partial CO_2 removal, and virtually complete H_2S, COS and NH_3 removal is 1.65 #/#coal.

The clean gas at 1150 ^{o}F, 500 psi, is expanded through a turbine to the fuel cell pressure level of 100 psi. This turbine supplies the compressor power of the air separation unit. Oxidant supply parasitic power is required for the motor driven, intercooled, oxygen compressor. Fuel gas leaves the turbine at 653 ^{o}F and is heated by a stream of anode outlet gas at 1300 ^{o}F to a mixture temperature of approximately

1120 ^{o}F for entrance into the fuel cell anode. In addition to heating the incoming fuel, the anode recirculation also establishes a carbon-free equilibrium mixture at the anode inlet.

The anode operates at a fuel utilization of .85. The anode discharge temperature is the fuel cell temperature of 1300 ^{o}F. From the anode discharge the vitiated fuel gas enters the catalytic burner which receives a portion of the discharge air for the gas turbine compressor. Air flow is 10.63 #/#coal which corresponds to 100% excess air. This has been selected at a level estimated to be close to a value for peak efficiency, based on the trade-off between fuel cell output, gas turbine output, and stack loss.

At the cathode inlet gas discharging from the catalytic burner mixes with air and gas recirculated from the cathode discharge through a steam generator heat exchanger. The recirculated flow is approximately 20 #/#coal.

Cathode inlet temperature is 1007 ^{o}F, and the discharge temperature is the fuel cell temperature of 1300 ^{o}F. The thermal duty of the recirculation flow heat exchanger is 16.7% of the coal HHV; the duty is superheating and reheating. The gas turbine pressure ratio is 6.18 with a turbine discharge temperature of 728 ^{o}F. The economizer downstream of the turbine adds heat to the steam in the amount of 11% of the coal HHV and its duty is feedwater heating.

This system has an efficiency (based on the assumption of no methane generation in the fuel cell) of .503 (6785 Btu/kWh). Some improvement may be expected in the final optimization of excess air, fuel cell pressure, gasifier pressure, and system parasitic losses (presently estimated at 9% of the net output).

For this cycle, we estimated plant performance under the assumptions that the fuel gas mixture equilibrates at the fuel cell anode inlet, and that methane formation is irreversible. This yielded an overall plant efficiency of .493 which compares with the value .503 (Table 3-11) calculated on the assumption that no methane is formed. Some adjustment of anode recirculation ratio was necessary to achieve this result.

Refer to Table 3-4 for flow sheet data, and Table 3-11 for overall performance data.

Table 3-4

CASE 1 OXYGEN-BLOWN SIMPLE TB 100% XSA

	P (psi)	T (^{O}F)	G lb gas / lb coal	O_2 (X_{O_2})	H_2 (X_{H_2})	N_2 (X_{N_2})	H_2O (X_{H_2O})	CO (X_{CO})	CO_2 (X_{CO_2})	CH_4 (X_{CH_4})	H_2S (X_{H_2S})	COS (X_{COS})	NH_3 (X_{NH_3})	Ar (X_{Ar})	H Btu / lb coal
1	600	2500	2.18	0	.2884	.0066	.1788	.4245	.0871	.0008	.0100	.0006	.0002	.0012	12018
2	500	1150	1.65	0	.3664	0	.0235	.5393	.0708	0	0	0	0	0	10158
3	100	1127	7.23	0	.1465	0	.1350	.2295	.4890	0	0	0	0	0	13234
4	99	1300	5.58	0	.0224	0	.1979	.0544	.7253	0	0	0	0	0	3670
5	99	1007	36.21	.1120	0	.6450	.0733	0	.1697	0	0	0	0	0	9195
6	98	1300	32.28	.0920	0	.7031	.0799	0	.1250	0	0	0	0	0	11716
7	98	1300	12.28	.0920	0	.7031	.0799	0	.1250	0	0	0	0	0	4457
8	14.7	60	10.63	.2100	0	.7900	0	0	0	0	0	0	0	0	0
9	100	492	10.63	.2100	0	.7900	0	0	0	0	0	0	0	0	1124
10	14.7	300	12.28	.0920	0	.7031	.0799	0	.1250	0	0	0	0	0	1101
11	98	1300	20.00	.0920	0	.7031	.0799	0	.1250	0	0	0	0	0	7258

We have selected this configuration as the reference cycle. Although its efficiency is somewhat lower than that of a fully cascaded cycle using a reheat gas turbine, it entails less risk in the high-temperature steam generator, and it utilizes a well-developed, commercially available gas turbine. The heat rate calculated on the assumption of no methane formation, is below the 6800 Btu/kWh goal.

Oxygen-Blown System with Partially Cascaded Bottoming Cycle (20% Excess Air).

Case 2. Calculation for this cycle has also been carried out for an excess air ratio of 20%. This results, as shown in Table 3-11, in a slight drop in fuel cell voltage and output (.1 point), a 2 point drop in gas turbine output, and a 1.8 point increase in steam output. The net results in a .3 drop in plant efficiency from the 100% excess air case. Flow sheet data appears in Table 3-5.

Oxygen-Blown System with Fully Cascaded Bottoming Cycle Using a Reheat Gas Turbine

Case 3. This cycle, in Figure 3-5, differs from the one described above in the following respects:

1. The fuel cell pressure is 150 psi, which results in a small contribution to the air separation compressor power (2% of coal HHV versus 2-1/2%). However, this results in a higher fuel cell voltage and a higher fuel cell exhaust heat content.

2. Heat rejected from the cathode recirculation stream is used for gas turbine reheat, the turbine being divided into high- and low-pressure sections with reheat to 1250 ^{o}F via a heat exchanger in the recirculation path. With this cycle the airflow is not subject to independent selection but is determined by the fuel cell temperature and cooling requirements. For the selected conditions, the excess air ratio is 190%. As a result of the additional gas turbine output resulting from the turbine reheat and higher airflow, and an acceptable ratio of steam cycle feedwater flow to turbine exhaust flow, this cycle has a higher efficiency than the partially cascaded cycle described above. The economizer performs feedwater heating and vaporization, leaving the superheating and reheating duty to the high temperature steam generator.

Reference to Table 3-11 shows the cycle efficiency as .517 at 150 psi fuel cell pressure. At 100 psi fuel cell pressure, the efficiency is approximately .514 due to a reduction in fuel cell voltage, and a reduction in gas turbine output which is less than compensated by an increase in steam output and reduction of parasitic power. Although this cycle has a higher efficiency than any of the other configurations, including the partially cascaded cycle, it is subject to two major disadvantages:

Table 3-5

CASE 2 OXYGEN-BLOWN SIMPLE TB 20% XSA

	P (psi)	T (^{o}F)	G lb gas / lb coal	O_2 (X_{O_2})	H_2 (X_{H_2})	N_2 (X_{N_2})	H_2O (X_{H_2O})	CO (X_{CO})	CO_2 (X_{CO_2})	CH_4 (X_{CH_4})	H_2S (X_{H_2S})	COS (X_{COS})	NH_3 (X_{NH_3})	Ar (X_{Ar})	H Btu / lb coal
1	600	2500	2.18	0	.2884	.0066	.1788	.4245	.0871	.0008	.0100	.0006	.0020	.0012	12018
2	500	1150	1.65	0	.3664	0	.0235	.5393	.0708	0	0	0	0	0	10158
3	100	1127	7.23	0	.1254	0	.1561	.2506	.4679	0	0	0	0	0	12986
4	99	1300	5.58	0	.0224	0	.1979	.0544	.7253	0	0	0	0	0	3633
5	99	1000	35.12	.0544	0	.5978	.1132	0	.2346	0	0	0	0	0	10207
6	98	1300	31.19	.0280	0	.6542	.1239	0	.1939	0	0	0	0	0	12078
7	98	1300	8.03	.0280	0	.6542	.1239	0	.1939	0	0	0	0	0	3377
8	14.7	60	6.38	.2100	0	.7900	0	0	0	0	0	0	0	0	0
9	100	492	6.38	.2100	0	.7900	0	0	0	0	0	0	0	0	674
10	14.7	300	8.03	.0280	0	.6542	.1239	0	.1939	0	0	0	0	0	1121
11	98	1300	23.16	.0280	0	.6542	.1239	0	.1939	0	0	0	0	0	9745

1. The technical risk of the high-temperature steam generator increases because of the more severe duty (superheating and reheating to the full temperature of the 2400/950/950 steam cycle).

2. The cycle requires the use of a reheat gas turbine, a complex machine which is not commercially available.

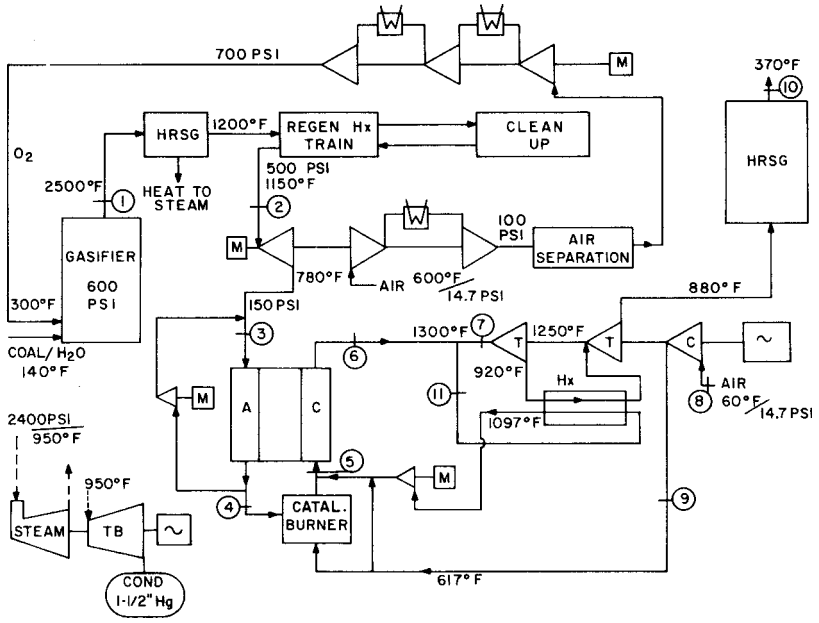

Figure 3-5. Oxygen-Blown System with Reheat Gas Turbine

Flow sheet data are shown on Table 3-6.

Using the methane formation assumption described in Oxygen-Blown System with Partially Cascaded Bottoming Cycle, plant performance falls to .507 with the fuel cell at 150 psi, after a suitable adjustment of the recirculation ratio is made.

Oxygen-Blown System with Regenerative Gas Turbine

Case 4. This cycle, in Figure 3-6, has the following distinguishing features:

1. The fuel cell operates at a pressure level of 50 psi, therefore, there is an excess of fuel gas expander turbine power delivered to the air separation compressor. This excess is absorbed by an alternator. The net oxidant supply power is reduced to .016 times the coal HHV.

2. The gas turbine is a regenerative machine in which the compressor discharge temperature is raised by heat exchange with the turbine exhaust to a level such that a cathode inlet temperature of 1037 °F can be main-

Table 3-6

CASE 3 OXYGEN-BLOWN RHTB 190% XSA

	P (psi)	T (^{O}F)	G lb gas / lb coal	O_2 (X_{O_2})	H_2 (X_{H_2})	N_2 (X_{N_2})	H_2O (X_{H_2O})	CO (X_{CO})	CO_2 (X_{CO_2})	CH_4 (X_{CH_4})	H_2S (X_{H_2S})	COS (X_{COS})	NH_3 (X_{NH_3})	Ar (X_{Ar})	H Btu / lb coal
1	600	2500	2.18	0	.2884	.0066	.1788	.4245	.0871	.0008	.0100	.0006	.0020	.0012	12018
2	500	1150	1.65	0	.3664	0	.0235	.5393	.0708	0	0	0	0	0	10158
3	150	1176	7.23	0	.1254	0	.1561	.2506	.4679	0	0	0	0	0	13890
4	149	1300	5.58	0	.0224	0	.1979	.0544	.7253	0	0	0	0	0	3938
5	149	1100	30.00	.1372	0	.6841	.0540	0	.1247	0	0	0	0	0	14928
6	148	1300	44.95	.1246	0	.7280	.0575	0	.0899	0	0	0	0	0	16473
7	148	1300	16.95	.1246	0	.7280	.0575	0	.0899	0	0	0	0	0	6207
8	14.7	60	15.3	.2100	0	.7900	0	0	0	0	0	0	0	0	0
9	150	617	15.3	.2100	0	.7900	0	0	0	0	0	0	0	0	2097
10	14.7	375	16.95	.1246	0	.7280	.0575	0	.0899	0	0	0	0	0	1963
11	148	1300	28.00	.1246	0	.7280	.0575	0	.0899	0	0	0	0	0	10267

tained without the need for cathode recirculation. The turbine exhaust temperature downstream of the regenerative heat exchanger is reduced to 426 °F, which is too low for any steam generation, expect the process steam for cleanup. The high-temperature steam generator produces all power generation steam. The efficiency of this cycle is .466 with a contribution of .03 from the steam cycle, and is .436 with no power generation steam contribution. The cycle's sole advantage is its simplicity (no cathode recirculation, and no economizer). It could be applied to a case in which the high-temperature steam generator is used to produce process steam at a modest temperature level.

Flow sheet data are shown in Table 3-7.

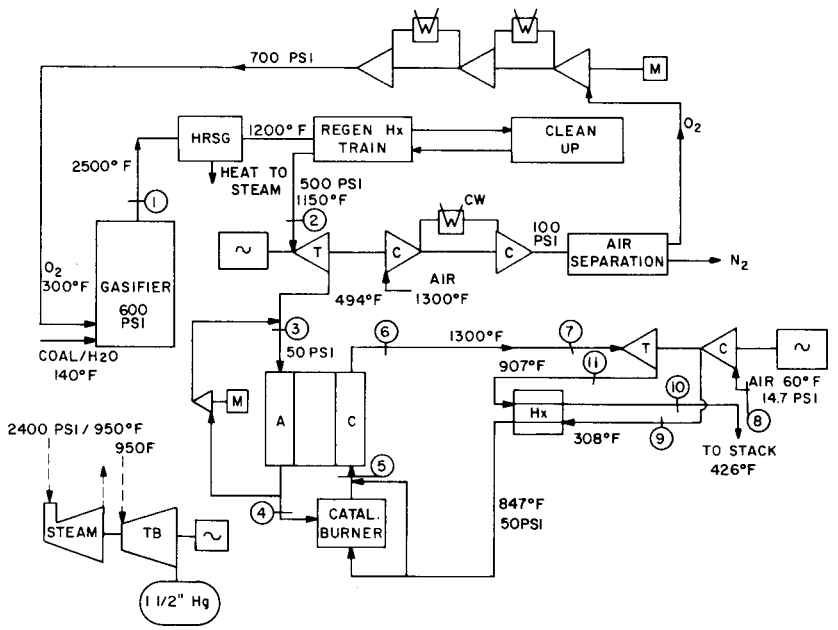

Figure 3-6. Oxygen-Blown System with Regenerative Gas Turbine

Air Blown Systems

Figures 3-7 and 3-8 illustrate air-blown systems. These include both fully and partially cascaded bottoming cycle. In these systems the blast temperature is achieved through heat of compression. We included these cycles in the scoping study to demonstrate the effects upon similar cycle configurations produced by a change in fuel source from an oxygen-blown gasifier to an air-blown gasifier.

Case 5. Figure 3-7 shows a system in which the gasifier blast temperature is reduced to 600 °F by use of an intercooler. Although this reduces parasitic power,

Table 3-7

CASE 4 OXYGEN-BLOWN REGEN TB 590% XSA

	P (psi)	T (^{o}F)	G lb gas / lb coal	O_2 (X_{O_2})	H_2 (X_{H_2})	N_2 (X_{N_2})	H_2O (X_{H_2O})	CO (X_{CO})	CO_2 (X_{CO_2})	CH_4 (X_{CH_4})	H_2S (X_{H_2S})	COS (X_{COS})	NH_3 (X_{NH_3})	Ar (X_{Ar})	H Btu / lb coal
1	600	2500	2.18	0	.2884	.0066	.1788	.4245	.0871	.0008	.0100	.0006	.0020	.0012	12018
2	500	1150	1.65	0	.3664	0	.0235	.5393	.0708	0	0	0	0	0	10158
3	50	1007	4.43	0	.1810	0	.1281	.3352	.3557	0	0	0	0	0	11790
4	49	1300	5.57	0	.0222	0	.1974	.0545	.7259	0	0	0	0	0	3929
5	49	1037	42.67	.1848	0	.1701	.0231	0	.0820	0	0	0	0	0	11246
6	48	1300	38.15	.1733	0	.7620	.0251	0	.0396	0	0	0	0	0	12925
7	48	1300	38.15	.1733	0	.7620	.0251	0	.0396	0	0	0	0	0	12925
8	14.7	60	36.50	.2100	0	.7900	0	0	0	0	0	0	0	0	0
9	49	308	36.50	.2100	0	.7900	0	0	0	0	0	0	0	0	2199
10	14.7	426	38.15	.1733	0	.7620	.0251	0	.0396	0	0	0	0	0	4072
11	15.3	907	38.15	.1733	0	.7620	.0251	0	.0396	0	0	0	0	0	8822

the effect of lower blast temperature on the gasifier fuel conversion ratio results in a loss of system performance.

Table 3-11 shows the overall plant performance as .458; Table 3-8, the flow sheet data.

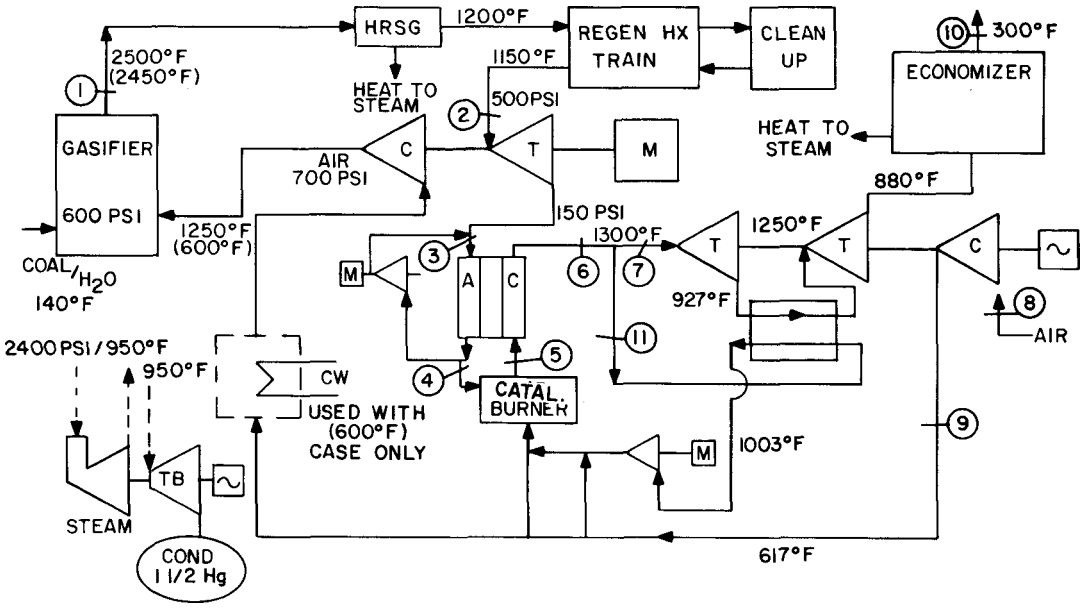

Figure 3-7. Air-Blown System with Reheat Gas Turbine (2 Cases)

Case 6. The same cycle as in Case 5, without the intercooler, achieves an air blast temperature to the gasifier of 1250 °F. The enhancement in gasifier performance and its resultant effect on fuel cell output exceeds the increasing air compressor power, and thus the plant efficiency is .491, 3 points higher than Case 5.

Flow sheet data appear in Table 3-9.

Case 7. Figure 3-8 illustrates a partially cascaded bottoming cycle system, with 1250 °F blast temperature. The efficiency is approximately 2 points lower than of the fully cascaded system at the same blast temperature, a result of the less efficient gas turbine cycle. Plant efficiency is .469; Table 3-10 shows flow sheet data.

Table 3-8

CASE 5 AIR-BLOWN RHTB 600°F BLAST 76% XSA

	P (psi)	T (°F)	G lb gas / lb coal	O_2 (X_{O_2})	H_2 (X_{H_2})	N_2 (X_{N_2})	H_2O (X_{H_2O})	CO (X_{CO})	CO_2 (X_{CO_2})	CH_4 (X_{CH_4})	H_2S (X_{H_2S})	COS (X_{COS})	NH_3 (X_{NH_3})	Ar (X_{Ar})	H Btu / lb coal
1	600	2450	6.89	0	.0858	.5333	.1514	.1275	.0904	.0002	.0043	.0003	0	.0068	13086
2	500	1150	5.72	0	.1052	.6541	.0138	.1562	.0707	0	0	0	0	0	8796
3	150	1085	14.33	0	.0425	.5887	.0646	.0928	.2114	0	0	0	0	0	12603
4	149	1300	8.62	0	.0129	.5352	.0844	.0192	.3483	0	0	0	0	0	4378
5	149	1050	15.51	.0917	0	.6614	.0517	0	.1952	0	0	0	0	0	4912
6	148	1300	30.81	.0507	0	.7734	.0605	0	.1154	0	0	0	0	0	11410
7	148	1300	12.61	.0507	0	.7734	.0605	0	.1154	0	0	0	0	0	4669
8	14.7	60	6.89	.2100	0	.7900	0	0	0	0	0	0	0	0	0
9	150	623	6.89	.2100	0	.7900	0	0	0	0	0	0	0	0	955
10	14.7	300	12.61	.0507	0	.7734	.0605	0	.1154	0	0	0	0	0	1248
11	148	1300	18.2	.0507	0	.7734	.0605	0	.1154	0	0	0	0	0	6741

Table 3-9

CASE 6 AIR-BLOWN RHTB 1250°F BLAST 109% XSA

	P (psi)	T (°F)	G lb gas / lb coal	O_2 (X_{O_2})	H_2 (X_{H_2})	N_2 (X_{N_2})	H_2O (X_{H_2O})	CO (X_{CO})	CO_2 (X_{CO_2})	CH_4 (X_{CH_4})	H_2S (X_{H_2S})	COS (X_{COS})	NH_3 (X_{NH_3})	Ar (X_{Ar})	H Btu / lb coal
1	600	2500	6.13	0	.1158	.4963	.1409	.1585	.0772	.0002	.0045	.0003	0	.0063	13908
2	500	1150	5.20	0	.1380	.6005	.0145	.1889	.0581	0	0	0	0	0	9991
3	150	1093	13.85	0	.0558	.5272	.0782	.1093	.2295	0	0	0	0	0	14163
4	149	1300	8.64	0	.0114	.4701	.1080	.0267	.3838	0	0	0	0	0	4710
5	149	1100	34.50	.0919	0	.7081	.0573	0	.1427	0	0	0	0	0	10642
6	148	1300	31.06	.0723	0	.7656	.0619	0	.1002	0	0	0	0	0	11535
7	148	1300	14.88	.0723	0	.7656	.0619	0	.1002	0	0	0	0	0	5527
8	14.7	60	9.68	.2100	0	.7900	0	0	0	0	0	0	0	0	0
9	150	623	9.68	.2100	0	.7900	0	0	0	0	0	0	0	0	1341
10	14.7	300	14.88	.0723	0	.7656	.0619	0	.1002	0	0	0	0	0	1492
11	148	1300	16.18	.0723	0	.7656	.0619	0	.1002	0	0	0	0	0	6008

Table 3-10

CASE 7 AIR-BLOWN SIMPLE TB 1250°F BLAST 50% XSA

	P (psi)	T (°F)	G lb gas / lb coal	O_2 (X_{O_2})	H_2 (X_{H_2})	N_2 (X_{N_2})	H_2O (X_{H_2O})	CO (X_{CO})	CO_2 (X_{CO_2})	CH_4 (X_{CH_4})	H_2S (X_{H_2S})	COS (X_{COS})	NH_3 (X_{NH_3})	Ar (X_{Ar})	H Btu / lb coal
1	600	2500	6.13	0	.1158	.4963	.1409	.1585	.0772	.0002	.0045	.0003	.0020	.0063	13908
2	500	1150	5.20	0	.1380	.6005	.0145	.1889	.0581	0	0	0	0	0	9991
3	150	1093	13.85	0	.0558	.5272	.0782	.1093	.2295	0	0	0	0	0	14164
4	149	1300	8.64	0	.0114	.4701	.1080	.0267	.3838	0	0	0	0	0	4710
5	149	1050	27.26	.0697	0	.6863	.0688	0	.1752	0	0	0	0	0	8254
6	148	1300	23.90	.0414	0	.7600	.0758	0	.1228	0	0	0	0	0	9161
7	148	1300	12.20	.0414	0	.7600	.0758	0	.1228	0	0	0	0	0	4677
8	14.7	60	7	.2100	0	.7900	0	0	0	0	0	0	0	0	0
9	150	623	7	.2100	0	.7900	0	0	0	0	0	0	0	0	970
10	14.7	300	12.20	.0414	0	.7600	.0758	0	.1228	0	0	0	0	0	1336
11	148	1300	11.70	.0414	0	.7600	.0758	0	.1228	0	0	0	0	0	4483

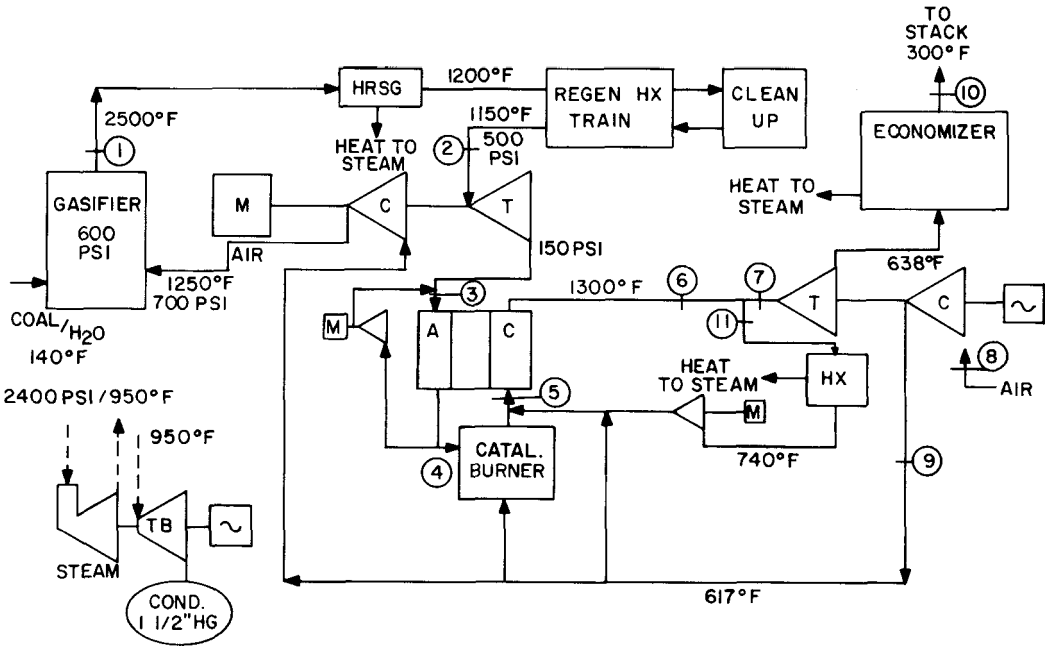

Figure 3-8. Air-Blown System with Partially Cascaded Bottoming Cycle

Summary. The air-blown systems show less fuel cell output per pound of coal than the oxygen-blown systems, but more gas turbine and steam outputs, the result of higher system mass flow and sensible heat content. System gross outputs, before parasitic power, compare favorably with the oxygen blown-systems, but net outputs are lower because of higher parasitic power for oxidant supply and for gas cleanup.

Detail system heat balance numbers are shown in Table 3-11.

Discussion of Scoping Study Results

Tables 3-11 and 3-12 summarize the comparative evaluations of the alternate cycles.

The oxygen-blown cycles have the following general advantages over the air-blown cycles:

1. Higher gasifier fuel conversion efficiency resulting in higher fuel cell output per pound of coal.

2. Lower oxidant supply parasitic power resulting from reduced oxidant total air flow requirement, relatively low pressure ratio of the air separation compressor, relatively low flow rate of oxidant required at 700 psi for gasifier injection, and use of oxidant supply compressor intercooling.

3. Lower product gas flow per pound of coal leads to reduced size of regenerative heat exchangers and gas cleanup components, consumption and lower cleanup parasitic power and process steam.

4. Higher positive pressure of contaminant gases and the cleanup absorber inlet.

5. Reduced fuel cell performance prediction uncertainty and corrosion risk, resulting from high H_2 concentration.

Table 3-11

ALTERNATE CYCLE ENERGY BALANCE SUMMARY

CASE #	1	2	3	4	5	6	7
	OX-BLOWN Simple TB 100% XSA	OX-BLOWN Simple TB 20% XSA	OX-BLOWN RH TB 190% XSA	OX-BLOWN Regen TB 590% XSA	AIR-BLOWN RH TB 600°F Blast 76% XSA	AIR-BLOWN RH TB 1250°F Blast 109% XSA	AIR-BLOWN Simple TB 1250°F Blast 50% XSA
GASIFIER ENERGY OUTPUT H_2+CO HHV Content	.767	.767	.767	.767	.565	.655	.655
Other Sensible/Latent Energy	.253	.253	.253	.253	.492	.481	.481
HRSG/DUCTING LOSSES	.01	.01	.01	.01	.01	.013	.013
HEAT DELIVERED TO STEAM (HT TEMP. HRSG)	.10	.10	.10	.10	.24	.23	.23
REGEN HX/CLEANUP HEAT LOSS	.08	.08	.08	.08	.10	.10	.10
CHEMICAL + SENSIBLE ENERGY AT REGEN HX CLEAN GAS OUTLET	.83	.83	.83	.83	.707	.793	.793
FUEL GAS EXPANDER INPUT TO OXIDANT SUPPLY COMPRESSOR	.025	.025	.02	.034	.051	.051	.051
FUEL CELL DC/AC VOLTAGE*	.78/.76	.77/.76	.78/.76	.74/.73	.79/.78	.80/.79	.80/.78
FUEL CELL OUTPUT	.399	.388	.339	.323	.256	.306	.305
GAS TB GEN OUTPUT	.069	.049	.119	.145	.130	.140	.108
HEAT DELIVERED TO STEAM IN BOTTOMING CYCLE	.278	.318	.184	0	.155	.180	.217
F.C./BOTTOMING CYCLE LOSSES NOT RETURNED TO GAS STREAM	.012	.012	.012	.007	.01	.01	.01
STACK LOSS	.107	.088	.156	.321	.105	.106	.102
STEAM TB GEN OUTPUT	.140	.158	.109	.030	.152	.155	.166
GROSS OUTPUT	.548	.545	.567	.498	.538	.601	.579
NET OXIDANT SUPPLY POWER	.020	.020	.025	.011	.05	.08	.08
OTHER PARASITIC POWER	.025	.025	.025	.021	.03	.03	.03
NET OUTPUT	.503	.500	.517	.466	.458	.491	.469
FIGURE #	4-4	4-4	4-5	4-6	4-7	4-7	4-8

NOTE: All values (except *) are fractions of HHV

For both oxygen- and air-blown systems the following advantages and disadvantages apply to the alternative bottoming cycle configurations:

Reheat Turbine Cycle. This cycle achieves the highest efficiency as a result of maximum cascading of fuel cell waste heat. This cascading must employ a ratio of steam (and feedwater) flow to gas flow such that a high percentage of gas turbine waste heat can be used in the high pressure reheat steam cycle. Its disadvantages are: (a) somewhat extreme duty requirement for the high-temperature steam generator

Table 3-12

COMPARATIVE EVALUATION OF SCOPING STUDY CYCLES

	OXYGEN-BLOWN SYSTEMS	AIR-BLOWN SYSTEMS	REHEAT GAS TB BOTTOMING CYCLE	PARTIALLY CASCADED BOTTOMING CYCLE	REGENERATIVE GAS TURBINE BOTTOMING CYCLE
ADVANTAGES	Highest Gasifier Fuel Conversion Efficiency Modest Blast Temp. Lowest Oxidant Supply Parasitic Power Highest Fuel Cell H_2 Conc. Lowest HX Size/Cost Lowest Cleanup Parasitic Power/Process Steam Highest Plant Efficiency	Relatively Simple Oxidant Supply Components	Provides Highest Plant Efficiency for Both Oxygen-Blown Plants (True Both with and Without Consideration of Methane Formation in the Fuel Cell)	Uses Simple Available Gas Turbine Minimizes Risk in Gasifier Discharge Steam Generator	Maximum Cycle and Component Simplicity Compatible with low Steam Flow and Pressure/ Temperature Requirement
DISADVANTAGES	Complexity/Cost of Air Separation and Oxygen Compression Components	Lower Fuel Conversion Efficiency Even at High Blast Temp. High Oxidant Supply Power High Cleanup Power/Steam High HX Cost Low H_2 Conc. in Fuel Cell Generally Lower Plant Efficiency	Complexity/Cost/ Unavailability of Reheat Gas Turbine Increased Gasifier Discharge Steam Generator Risk	1-2 Pts Lower in Plant Efficiency Than RH Gas Turbine Cycle	4-5 Pts Lower in Plant Efficiency Than Highest Efficiency Alternate Cycle

(final superheat + reheat) and, (b) use of the complex high cost reheat gas turbine which is not commercially available.

Partially Cascaded Bottoming Cycle. This cycle is somewhat below the reheat turbine cycle (.1 to .2 pts) for both air- and oxygen-blown systems. However, it is free of the above cited disadvantages of the latter cycle. Increase in excess air from 20% to 100% (oxygen system) increases the fuel cell output very slightly (.1 pt), increases gas turbine output, and reduces steam output. The net increase in plant efficiency is .3 pt.

Regenerative Gas Turbine Cycle. This cycle suffers an efficiency loss from the alternative because of the inherent mismatch between gas turbine discharge gas flow and steam (feedwater) flow, which results in a high stack temperature and low heat input to the steam. Also, fuel cell output suffer from very high excess air (590%) and from the effect of the low gas turbine pressure ratio.

The offsetting advantage is cycle simplicity (no cathode recycle) and no steam generator heat exchanger other than the high-temperature steam generator. This cycle might be attractive for an application requiring low-pressure/temperature steam, which would result in minimum risk gasifier discharge steam generator.

REFERENCES

1. Economic Studies of Coal Gasification Combined Cycle Systems for Electric Power Generation. Fluor Engineers and Constructors. EPRI Report # AF-642, January 1978.

2. Letter. Texaco Development Corporation to General Electric Company, June 20, 1977.

3. Physical and Thermodynamic Properties of Elements and Compounds. Chemtron Corporation (Computerized by GE).

Section 4

OIL-FIRED POWER PLANT STUDIES

INTRODUCTION

The oil-fired power plant represents the second category of plant included in the present evaluation. The category addresses small, distributed installations where minimum capital cost, prompt response characteristics and minimum environmental intrusion are desired characteristics. Major plant components are reduced to the fuel processing subsystem, which produces a clean H_2+CO fuel from a heating oil feedstock, and the fuel cell/power conditioning energy conversion subsystem. The requirements for small size and minimum capital cost have eliminated, at least initially, consideration of waste heat bottoming cycles. Consequently, the distributed oil-fired power plant provides a significant amount of heat energy which could be made available to a local customer for space or process heating. In quoting power plant performance, this "co-generation" heat receives no credit.

POWER PLANT REQUIREMENTS AND GOALS

Table 4-1 lists general design requirements and goals for the oil-fired power plant. The specified fuel is No. 2 heating oil of the composition given in Table 4-2.

Table 4-3 lists existing environmental limits applicable to the oil-fired power plant, along with projected limits for the 1985 time period. We used these projected standards as the design basis for the reference oil-fired plant.

As shown in Table 4-1, heat rate and capital cost of 7500 Btu/kWh and $300/kW(e), respectively, along with an availability of 90%, are the targets for the oil-fired plant. Table 4-4 summarizes the control goals for the intermediate load oil-fired plant.

Table 4-1

GENERAL DESIGN REQUIREMENTS AND GOALS
FOR THE OIL-FIRED POWER PLANT

Requirements

1.	Dispersed Station Plant (Industrial Application)	
2.	Power Level	4 - 5 MW(e)
3.	Fuel	No. 2 Fuel Oil
4.	Site Characteristics	"Middletown" Modified for Industrial Application
5.	Environmental	Projected 1985 Federal Requirements

Goals

1.	Intermediate Load Duty with Hourly* Load Following Capability	
2.	Heat Rate	7500 Btu/kWh
3.	Installed Capital Cost (1978)	$300/kW(e)
4.	Plant Availability	90%
5.	Life (50% Capacity Factor)	
	Fuel Cell Stacks	9 Years
	Balance of Plant	30 Years

*1 minute response from 25% to 100% of load

Table 4-2

COMPOSITION OF NO. 2 FUEL OIL

	%
Ash	.01
Sulfur	0.22 Max
Hydrogen	12.60
Carbon	87.30
Nitrogen	.006
Oxygen	.04
Higher Heating Value	19280 Btu/lb

Table 4-3

CURRENT AND PROJECTED EMISSIONS STANDARDS FOR THE OIL-FIRED PLANT

Pollutant	Current Standards	Projected 1985 Federal Requirements
SO_x	0.8 lb/10^6 Btu	0.2 lb/10^6 Btu
NO_x	0.3 lb/10^6 Btu	0.15 lb/10^6 Btu
TSP	0.1 lb/10^6 Btu	0.03 lb/10^6 Btu

Table 4-4

CONTROL GOALS FOR THE
INTERMEDIATE LOAD OIL-FIRED PLANT

1. Daily Load Following

   - Able to load and unload up from 25 to 100% of nameplate MW rating in 1 minute or less
   - Module shutdown not required

2. Startup/Shutdown

   - Startup: Cold startup in 2 hours; hot startup in 1 hour
   - Shutdown: 100% to zero load in 1 hour

3. Frequency Governing

   - Respond +1.3% - 0.7% of unit nameplate rating in seconds in prompt, stable fashion
   - Maximum deadband of .06% frequency
   - Maximum overall steady-state regulation of 5%

4. Abnormal Conditions

   - Complete load rejection (breakers opening)
   - Partial load rejection (from power system breakup)
   - Sustained abnormal voltage or frequency operation

OIL-FIRED POWER PLANT STUDIES

Plant Description

Early in the program we identified and studied in detail an oil-fired power plant system concept. The system concept we selected for study was based on a review of published work by other contributors in the field and by in-house subsystem evaluations. The work performed by Catalytica Associates for EPRI (1) was influential in the plant selection.

The objectives of the oil-fired plant evaluation were:

1. To perform an independent performance assessment for comparison with the performance goal of 45.5% overall efficiency;

2. To establish a performance benchmark for comparison with later evaluation of system parameters and subsystem options;

3. To quantify the influence of specific subsystem performance and operating limitations on overall plant efficiency and operation;

4. To evaluate specific plant operating parameters and subsystem alternatives as the basis for selecting a reference plant configuration for further technical and economic evaluation.

Referring to the power plant schematic in Figure 4-1, one then sees that the oil-fired system consists of three major components interconnected by means of miscellaneous piping, heat exchangers, pumps and a knockout drum condenser:

- Autothermal Reformer
- Gas Cleanup
- Molten Carbonate Fuel Cell

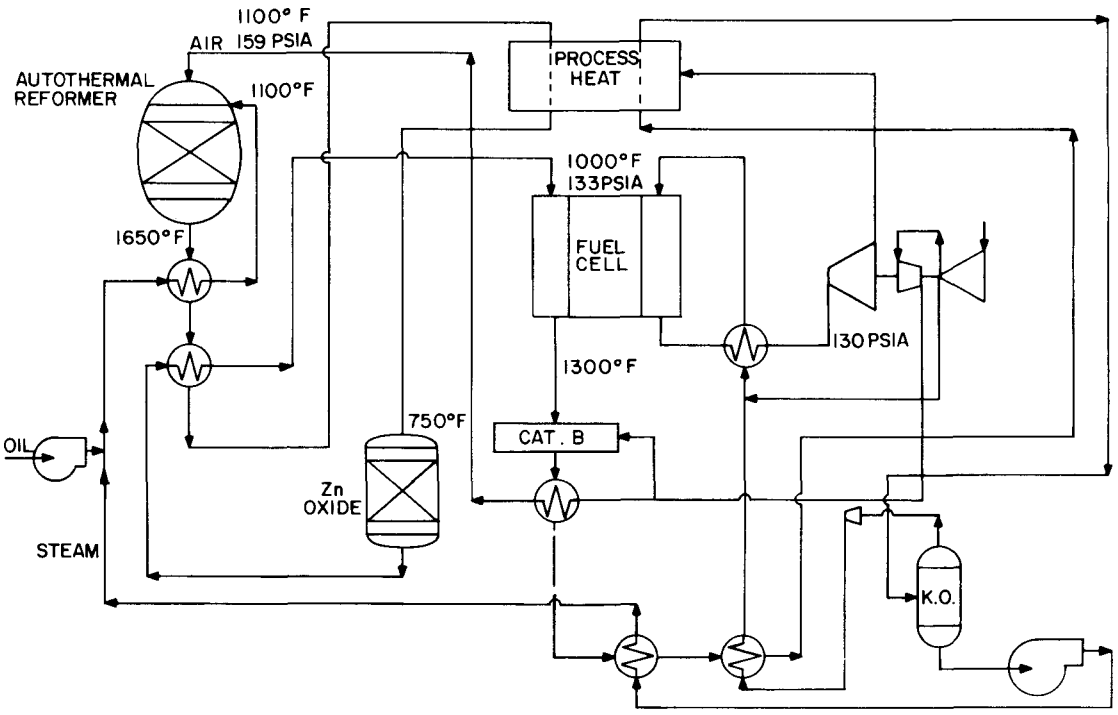

Figure 4-1. Oil-Fired Fuel Cell Power Plant

We selected the autothermal reformer because it is less developmental than other reformer options, and, thereby, is more likely to become available within the timeframe of the molten carbonate fuel cell development program. A zinc oxide polisher was selected for gas cleanup (sulfur removal) because of its simplicity and low capital cost compared to other gas cleanup processes.

The plant also includes heat recovery heat exchangers, located where they can utilize practical waste heat, and thereby increase overall plant efficiency. The unrecovered waste heat is made available for local consumers, achieving the fullest possible utilization of the energy content of the fuel. The catalytic burner is chosen to achieve complete consumption of the fuel energy not utilized in the fuel cell. An expansion turbine is incorporated to make up auxiliary power losses for pumping and air compression. The knockout drum condenser is employed to remove sufficient water from the spent fuel gas to achieve zero overall water consumption at normal operating conditions.

The fuel (No. 2 Oil), as shown in the diagram, mixes with steam, and passes through a heat exchanger where the mixture heats to 1100 ^{o}F. The steam oil mixture is then fed into the autothermal reformer. The heat used to raise the temperature of the mixture is extracted from the reformer exit gas, and the heat used to generate the steam is extracted from the fuel cell anode exit gas.

The autothermal reformer is also fed by 1100 ^{o}F air which is heated by fuel cell anode gas. The mixture of steam and oil vapor reacts with the air in the autothermal reformer and the product gas exits at 1650 ^{o}F. The hot gas cools to 750 ^{o}F and passes through a zinc oxide polisher where the sulfur compounds are chemically removed from the fuel gas. The clean fuel gas then recirculates through a heat exchanger where hot fuel from the autothermal reformer reheats it to 1100 ^{o}F.

This hydrogen-rich gas is fed into the anode side of the fuel cell which operates at 133 psia. Meanwhile, the cathode side of the fuel cell is fed with 1000 ^{o}F air and part of the anode exhaust gas which has been heated with hot exhaust gas from the fuel cell. The hydrogen and carbon monoxide content of the fuel gas reacts with oxygen and carbon dioxide in the fuel cell's cathode to create electrical power which in turn is converted to alternating current using inverters. The heat is extracted from the fuel cell by the anode and cathode exhaust gases. The hot cathode exhaust gas releases much of its heat content to the cathode inlet gas and then exits the system through an auxiliary power turbine. The anode exhaust gas

passes through a catalytic burner which burns the remaining combustibles. The hot exhaust from the burner cools and passes to the knockout drum where the entrained water condensate is separated for reuse. The condensed water starts its cycle over again by being vaporized and routed back to mix with the incoming fuel. The balance of the cold anode exhaust gas exist the knockout drum, mixes with compressed air and reheats to 1000 ^{o}F. The mixture, rich in oxygen and carbon dioxide, is fed to the cathode side of the fuel cell where much of the oxygen and carbon dioxide is consumed.

The fuel cell module, consisting of multiple stacks, is assumed to be a single, factory assembled, self-contained pressure vessel. Although there is conceptual commonality with the individual modules chosen in the coal-fired plants, current differences in operating pressure, method of heat rejection, and fuel gas heating value (amount of heat rejection) are significant.

Plant Performance

Uniform fuel cell analyses methods, described in Section 5 and used in the coal plant studies, provided a consistent treatment of fuel cell performance. In particular, the fuel cell model allows the prediction of the voltage versus current density characteristic as a function of fuel gas composition and operating pressure. A number of unifying assumptions, identical to those made for the coal-fired studies, were applied to the fuel cell subsystem. These were summarized as follows:

- Water-gas shift equilibrium is maintained at all points within the fuel cell;
- Methane present in the fuel gas does not participate in the cell reactions;
- Polarization voltage drop is defined as 0.7 Ωcm^2;
- Anode utilization is 0.85;
- Anode and cathode inlet temperatures are 1000 ^{o}F;
- Anode and cathode exit temperature is 1300 ^{o}F;
- Cell heat rejection is accomplished by excess air flow to the cathode;
- dc to ac inverter efficiency is 0.98;
- Fuel cell design point is specified by setting a fixed value of current density, taken here to be 161.5 mA/cm^2 for cell fuel concentrations considered.

By assumption of a fixed "design" value of current density, the voltage is allowed to vary with fuel composition. Eventual optimization of the fuel cell operating conditions will probably favor maximum power output (wattage) versus system cost. However, at this stage of comparative system evaluation, we judged it appropriate to specify the fuel cell on the basis of a constant loss mechanism.

We calculated the reformer performance and composition using a standard chemical equilibrium program. CHEMICAL EQUILIBRIUM ANALYSIS in Section 5 describes this method in detail and produced a good match with published literature (1). Initial reformer analyses were based on determining a carbon to water weight ratio (4.0) from literature (1) and iteratively adjusting the air feed rate to achieve the desired exit temperature. The exit temperature was kept low enough (1650 ^{o}F) to achieve good efficiency and high enough to avoid fouling the catalyst with sulfur. The reformer heat loss was assumed at 1%.

Development of the above methodology for chemical analysis made it possible to define and to calculate reformer and fuel cell performance and operating conditions, as shown in Table 4-5, and to identify potential system-wide chemistry problems, such as reformer sooting, carbon formation, methane formation and fuel cell chemical poisoning, which need further evaluation.

Based on the fuel cell and reformer analysis methods and standard calculation of the turbine output and parasitic power losses, we calculated the system's performance, as shown in Table 4-6. Table 4-7 gives the material and energy balance for the oil-fired plant and Figure 4-2 shows the energy flows in a schematic diagram. As Table 4-6 depicts, the system does not meet the goal of 45.5% efficiency. Our studies show that significant improvement might be made in reformer efficiency which would cause a parallel improvement in fuel cell (and power plant) efficiency.

There are analytical methods for studying both carbon and methane formation; these methods were adapted to computer use and are discussed in CHEMICAL EQUILIBRIUM ANALYSIS. These analyses are based on chemical equilibrium with the provision that gas temperatures exceed 500 ^{o}C and are thereby conservative. We judge that kinetic approach to equilibrium will not occur except when sufficient residence time (order of seconds) above approximately 500 ^{o}C is available in the presence of a catalyst. These conditions are most notably met in the anode passages of the fuel cell. Analysis indicates that, as a consequence of fuel gas composition, the oil-fired plant will not have a carbon deposition problem. However, the potential for methane formation does exist, and this problem needs quantitative, experimental evaluation.

Table 4-5

REFORMER AND FUEL CELL PERFORMANCE -- OIL-FIRED PLANT

Reformer Efficiency $\frac{HHV_{H_2+CO}}{HHVoil}$	0.946
Fuel Gas HHV_{H_2+CO}	2640 Btu/lb of gas
Reversible Cell Potential @ 0.85 Anode Utilization Counterflow	0.923V
Operating Voltage @ 161.5 mA/cm^2	0.810V
Fuel Cell Efficiency $\frac{Elec.\ Energy}{HHV_{H_2+CO}}$	0.4675

Table 4-6

OIL-FIRED POWER PLANT PERFORMANCE

Oil Feed (lb/hr)	1842 lb/h
MW(th)	10.40 MW(th)
Net Power Output	4.5 MW(e) ac
Plant Efficiency (%)	43.3 %
Plant Heat Rate (Btu/kWh)	7890 Btu/kWh

Table 4-7

OIL-FIRED PLANT MATERIAL AND ENERGY BALANCE

Stream Number	1	3A	2B	4	10	11	21	22	23	24
Stream ID	OIL	STEAM	AIR TO REFORMER	REFORMER EXIT	ANODE INLET	ANODE EXIT	CATHODE INLET	CATHODE EXIT	TURBINE INLET	VENT
Temperature (^{O}F)	77	575	1100	1650	1000	1300	1000	1300	770	250
Pressure (psia)	14.7	162	159	149	134	133	134	133	130	15
Gas Composition (Mole Fraction)										
O_2			.2100	0	0	0	.1641	.1450	.1450	.1450
CO				.1337	.1337	.0205	.0000	.0000	.0000	.0000
H_2				.2899	.2901	.0262	.0000	.0000	.0000	.0000
CO_2				.0718	.0718	.3954	.1065	.0432	.0432	.0432
CH_4				.0012	.0012	.0009	.0000	.0000	.0000	.0000
N_2			.7810	.3020	.3020	.2220	.6875	.7651	.7651	.7651
A_R			.0090	.0035	.0035	.0026	.0079	.0088	.0088	.0088
H_2S				.0002	.0000	.0000	.0000	.0000	.0000	.0000
H_2O		1.0000		.1977	.1977	.3324	.0341	.0379	.0379	.0379
Total Flow $\frac{lb\ mol}{hr}$		202.18	249.80	646.48	646.58	879.34	3442.15	3092.82	3092.82	3092.82
Total Flow lb/hr	1841.63	3642.56	7234.25	12718.13	12714.08	26692.72	103709.57	89729.56	89724.56	89724.56
Enthalpy Flux $\frac{MBtu}{hr}$	35.507	4.64	1.85	44.41	40.88	20.98	26.69	30.94	17.92	6.09

The selective concentration of residual fuel-borne sulfur compounds within the fuel cell electrolyte, identified in Section 2 as a potential system problem, has not been specifically examined for the oil-fired plant. This potential problem is treatable via system changes, such as partial venting of the anode exhaust stream prior to re-injection into the cathode.

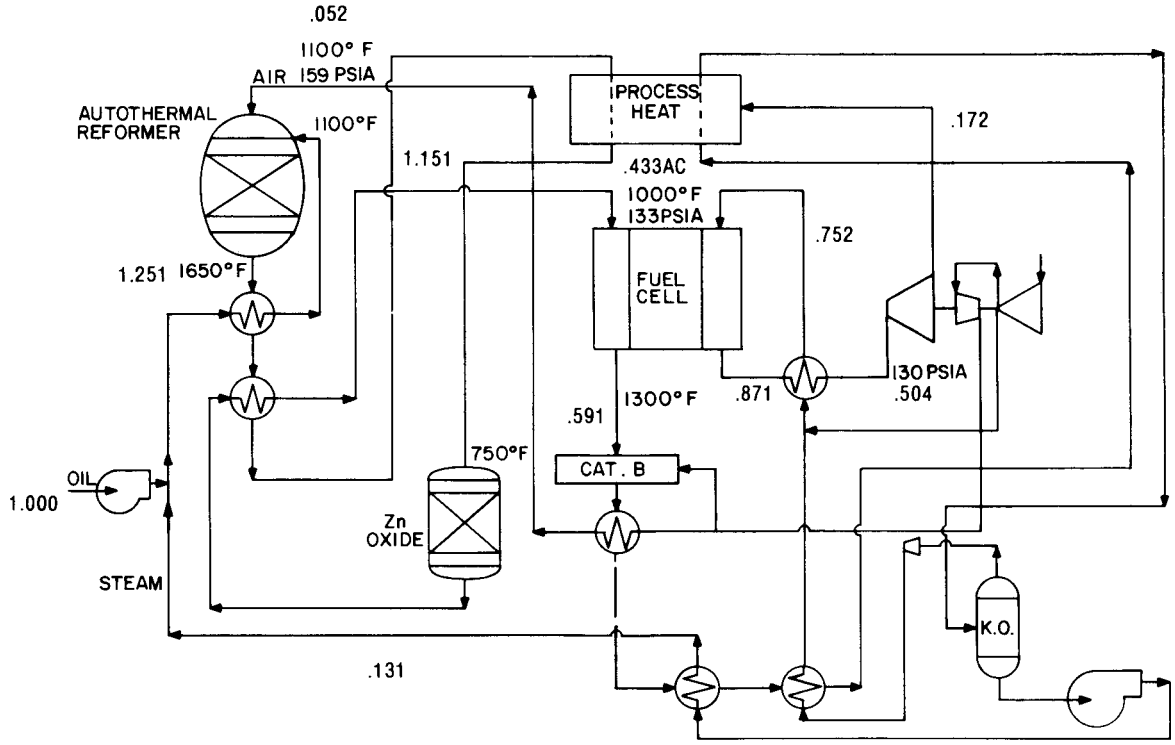

Figure 4-2. Energy Flows, Oil-Fired Fuel Cell Power Plant

OIL-FIRED POWER PLANT EFFICIENCY IMPROVEMENT

Based on study of the plant, one can formulate straight forward principles for the evaluation of fuel cell power plants without steam cycles. The efficiency of any fuel cell power plant with zero net bottoming cycle output is directly proportional to the efficiencies of the oil reformer, fuel cell, and inverter.

$$\eta_{plant} = \eta_{reformer} * \eta_{fuel\ cell} * \eta_{inverter} + \frac{XT - Losses}{Oil\ HHV} \qquad (1)$$

Expansion turbine bottoming power (XT) could theoretically be increased to produce net output power beyond the parasitic losses (Losses) due to pumping an air com-

pression; however, since the fuel cell module is more efficient and has much higher electric output than an expansion turbine, the determination of optimum plant operating conditions (except for pressure) should maximize fuel cell output. In this case the efficiency of the plant is simply the product of the component efficiencies.

$$\eta_{plant} = \eta_{reformer} * \eta_{fuel\ cell} * \eta_{inverter} \qquad (4\text{-}2)$$

Since the dc to ac inverter efficiency is constant (an assumed 0.98 for this study), only the fuel cell efficiency and/or reformer efficiency can increase the power plant efficiency. Similarly, we have assumed aggressive values of anode utilization and current density for the fuel cell. Thus, one finds the most potential for further improvement in overall plant efficiency in the oil reforming process. It is desired to improve the fuel gas conversion efficiency through greater utilization of power plant excess sensible heat. This approach not only increases the fraction of input energy available for fuel cell use, but also increases fuel cell voltage (and hence power) by a corresponding increase in the fuel heating value.

Within limits variation of the cathode inlet stream composition is possible. Composition of the cathode inlet gas stream is a function of anode stream and oxidant composition, flow rate, and system configuration.

Specific changes in the system configuration can affect cathode composition. Anode recirculation, cathode recirculation or a combination of the two are viable alternatives to cooling the fuel cell with air. Preliminary analyses have shown that fuel cell cooling via cathode recirculation is preferable to anode recirculation because of improved fuel cell efficiency. However, based on scoping calculations, the estimated impact of these system changes on fuel cell efficiency is small. The use of oxygen rather than air seems intuitively inconsistent with economics except for a baseload duty power plant. The most effective way to increase fuel cell efficiency is to improve the chemical composition of the fuel cell anode inlet gas stream, i.e., higher hydrogen and carbon monoxide content.

Irrespective of the reforming process, the efficiency of a reformer in a fuel cell power plant is determined only by its production of hydrogen and carbon monoxide. Thus, the term "reformer efficiency," as used in this study, is defined below, where HHV is high heating value.

$$\eta_{reformer} = \frac{(H_2+CO)\ HHV}{Oil\ HHV} \qquad (4\text{-}3)$$

The autothermal reformer exit temperature is kept as low as possible in order to keep methane content at the minimum practical level. However, sulfur tolerance of the reformer catalyst is greater at high temperatures. A temperature of 1650 ^{o}F is the estimated minimum reformer exit temperature consistent with catalyst reliability in the presence of sulfur.

If autothermal reforming is used to gasify the oil, then a reduction of the air flow to the reformer can increase the efficiency of the reformer. Reducing the air flow causes less heat generation in the reformer via combustion, and an increase of the sensible heat content of the inlet constituents, oil, steam and air must compensate for the loss in combustion heat. In these studies the oil and steam are mixed before preheating in order to reduce the possibility for coking. Even so, there is a temperature limit to which the mixture can heat without coking. This limit, based on available data for similar fuels, is an estimated 1100 ^{o}F. Thus, the loss in combustion heat caused by reducing the air feed rate must be substantially compensated by increasing the heat content of the air.

The first step in evaluating reformer efficiency improvement was to establish the limits with which sensible heat can be substituted in place of combustion. In a system installation, reformer performance is limited by the peak temperature available for heating the air (about 1750 ^{o}F at the catalytic burner exit). However, a more severe limitation on reducing the fraction of fuel combusted is carbon deposition, found in experimental work with heavy oil fuel feedstocks. Carbon deposition in the reformer causes soot to form on the catalyst, leading to eventual catalyst inactivity. The soot problem establishes an empirical, state-of-the-art limit on the improvement in reformer performance as summarized in Figure 4-3. The data points shown represent data produced by JPL (2) in autothermal reformer development. Although the precise value of this experimental minimum air condition is not well defined, its value appears to be in the range of 1.6 to 1.8 air to carbon molar ratio, as depicted in Figure 4-3. The figure also shows the theoretical soot deposition boundaries as calculated by General Electric and by JPL (2). The premature occurrence (in terms of decreasing air/carbon ratio) of an experimental soot boundary relative to the equilibrium prediction is noteworthy. Additionally, a large increase in steam/carbon ratio does not appear to help. This implies that the sooting problem is the result of fuel decomposition (cracking) or heterogeneous partial oxidation. The significant conclusion is that a more restrictive soot limit exists in practice than in theory. Figure 4-3 also shows as a circled point, that the autothermal reformer prediction for the oil-fired plant is on the carbon-free side of the experimental boundary.

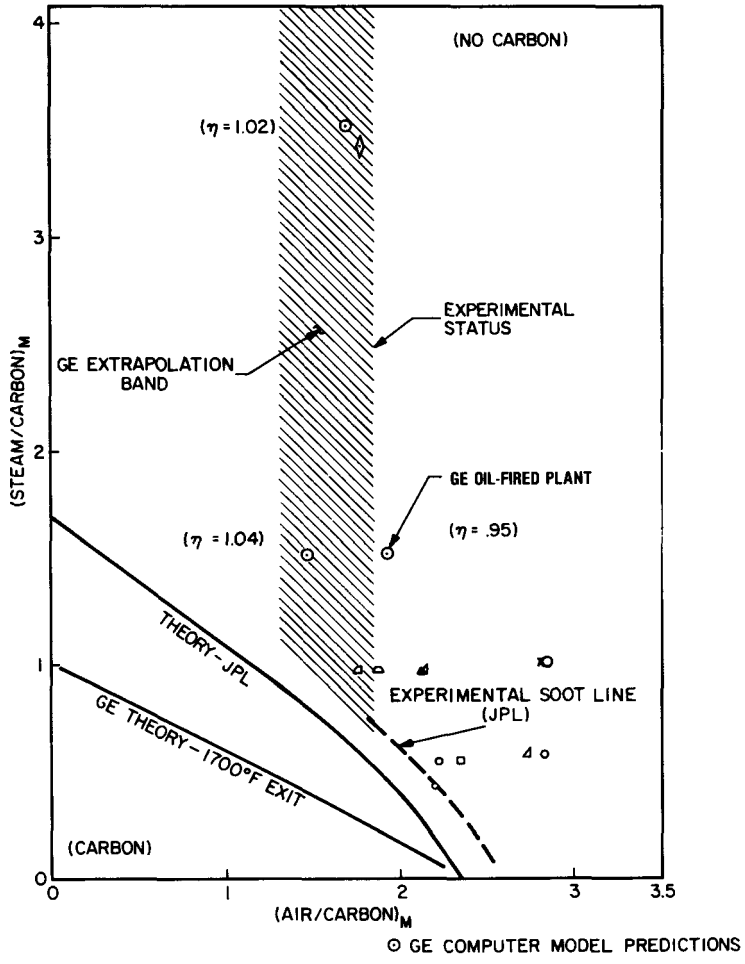

Figure 4-3. Autothermal Reformer Soot Line

The effect of variations in air/carbon and steam/carbon ratio on autothermal reformer conversion efficiency has been predicted using the analytical technique described in AUTOTHERMAL REFORMER in Section 5. Figure 4-4 shows the quantitative results of varying the reformer inlet flows for an operating pressure of 65 psia. A reformer exit temperature of 1650 ^{o}F was maintained for all cases by suitable selection of preheat temperatures.

Reformer efficiency increases markedly with reduced air flow, to attain values well over 100% for a steam to carbon ratio of 1.5. However, at high reformer efficiencies, the air to carbon ratio is well into the potential soot region of the reformer as discussed above. Although the soot problem is theoretically solvable via improved mixture control, current test experience has not been successful at the desired levels of air to fuel ratios. Reformer conversion efficiency is currently limited

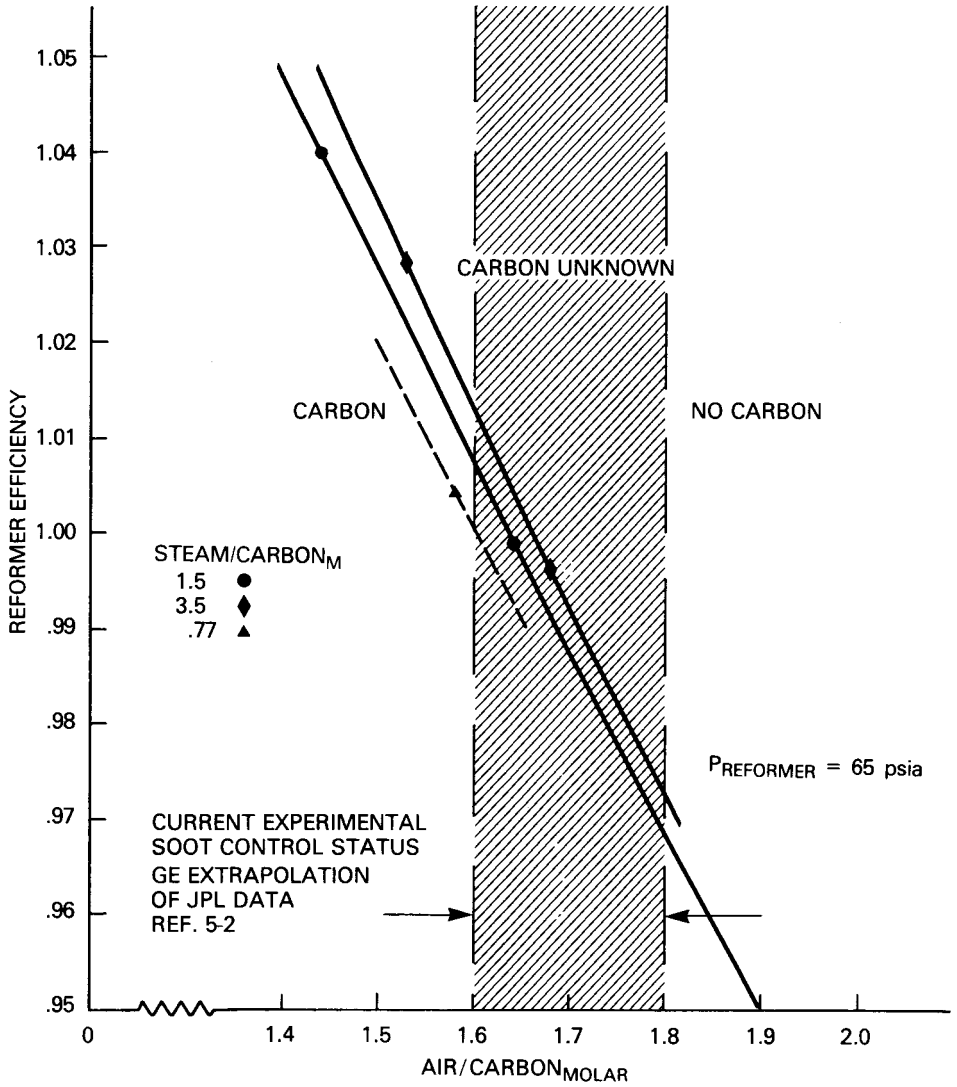

Figure 4-4. Oil Reformer Efficiency, 1650 ^{o}F Ref. Exit. Temp.

to 0.98 - 0.99. Figure 4-4 also shows an increase in reformer efficiency as a function of steam flow; increasing the stream flow gives a substantial improvement in reformer efficiency.

The integrated power plant performance was evaluated as a function of reformer operating parameters using equation 4-2 where the fuel cell electric efficiency is defined by the equation below:

$$\eta_{\text{fuel cell}} = \frac{\text{dc power output}}{\text{anode inlet gas HHV } (H_2+CO)} \qquad (4\text{-}4)$$

Figure 4-5 shows the calculated power plant performance as a function of reformer operating parameters for a plant with a reformer pressure of 65 psia. As the reformer efficiency is increased by a reduction of the reformer air flow, fuel cell efficiency also increases because of the improvement in anode inlet gas composition. However, Figure 4-5 indicates that the reformer efficiency needed to achieve the power plant efficiency goal of 45.5% is beyond current test experience in successfully controlling soot formation in the reformer. The figure also shows the effect of steam flow on power plant performance. Although increasing the reformer steam flow enhances reformer efficiency and soot control, fuel cell efficiency suffers significantly with steam flow because the increase in steam reduces the concentrations of hydrogen and carbon monoxide in the anode inlet gas. As reformer air flows are reduced to values needed to achieve the power plant efficiency goal, reformer efficiency becomes insensitive to steam flow. Hence, the loss in fuel cell efficiency is greater than the gain in reformer efficiency with increased steam flow. The optimum steam flow is less than considered in the study and is likely defined by the minimum steam flow needed to avoid carbon deposition in the reformer.

It should be noted that while the absolute values of reformer and plant efficiencies shown in Figures 4-4 and 4-5 apply specifically to a plant configuration in which the reformer operates at 65 psia, the trends and magnitude of change are equally applicable to the plant described which operates with the reformer at 150 psia.

Clearly, for any given air to fuel ratio, the optimum reformer steam to fuel ratio is unique and determinable by a straightforward parametric calculation. However, reformer (and power plant) optimization studies cannot be performed without establishing or assuming the lower limit for air to fuel feed ratio based on reformer soot control. Provided that reasonable improvement can be made in autothermal reformer soot control, the efficiency of an oil-fired, fuel cell power plant can be improved to meet the study goals.

Since reformer optimization is the most effective way to improve power plant efficiency and since current autothermal development has encountered performance limitations due to carbon formation (soot), alternate reforming methods are worthy of consideration. The possible processes for converting No. 2 oil to a gaseous fuel are these three options: Autothermal reforming, high temperature steam reforming, and newer hybrid processes such as the KTI process. Other processes, such as conventional steam reforming, have limitations, notably sulfur tolerance. Both

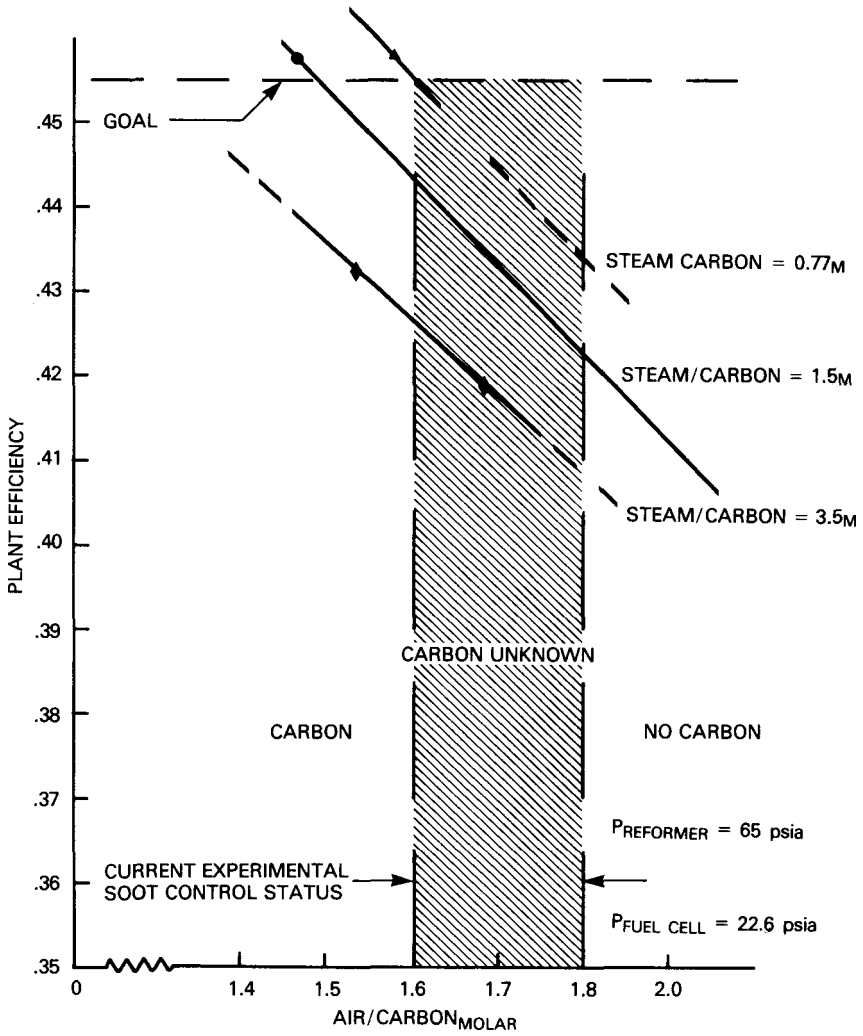

Figure 4-5. Oil-Fired Power Plant Efficiency

the autothermal reformer and the high temperature steam reformer are judged capable of processing No. 2 oil without desulfurization. Where the autothermal reformer has demonstrated some immunity to carbon deposition problems in test conditions, testing of certain high-temperature steam reformers has revealed a more severe carbon deposition problem (1). The hybrid process, consisting of a Toyo steam reformer followed by an autothermal reformer, is being investigated as an alternative approach to processing high sulfur content fuels. The apparent ability of the two stage hybrid process to tolerate (and gasify) solid carbon deposits may allow near-term realization of fuel gas conversion efficiency greater than 1.0.

Although both the autothermal reformer, the high-temperature steam reformer, and the hybrid process are judged to have the potential for load following and unat-

tended operation, the autothermal reformer clearly has superior design simplicity and thermal response characteristics because of its large single vessel configuration as opposed to the multi-tube configuration contained in a steam reformer vessel. Assuming no bottoming cycle power generation, the high temperature steam reformer would have the potential for superior thermal efficiency because theoretically the waste heat from the molten carbonate fuel cell might be used as the heat source for the reformer. While the high temperature steam reformer has certain theoretical advantages, the autothermal reformer can nonetheless be competitive while entailing lower development risk and less expensive design. An economic trade-off between these two reformers would be based on the reduced operating cost resulting from superior plant efficiency.

REFERENCES

1. Assessment of Fuel Processing Alternatives for Fuel Cell Power Generation. Palo Alto, Calif.: Electric Power Research Institute, October 1977. EM-570

2. John Houseman. "Autothermal and Steam Reforming of Distillate Fuel Oils" in National Fuel Cell Seminar Abstracts. July 1978, pp. 134-136.

Section 5

ANALYSIS MODELS

MODELING REQUIREMENTS

Analytical models and computer simulation of several significant plant subsystems serve as useful tools to provide information on the fundamental process behavior and characteristics of these fuel cell plant components.

The models utilized during the study include calculations for the gasifer reformer and fuel cell subsystem, as well as several general purpose analytical tools (such as limited species chemical equilibrium model and a carbon formation evaluation). The latter are used as sub-parts of the major models and provide analytical tools for application to specific portions of the cycle evaluation, as appropriate.

The use of these tools provides insight, aids understanding of the fundamental process behavior, and indicates the impact of a number of process interactions between major plant components.

FUEL CELL SUBSYSTEM MODEL

Introduction

Model Development Motivation. A lumped parameter model of the fuel cell subsystem has been developed for incorporation in the simulation of the overall plant. We used the resultant computerized representation to calculate the cycle energy and mass balance, power output, efficiency and sensitivity to variations in plant operating parameters. As part of the study, the simulation provides a convenient means to explore the impact of the fuel cell subsystem configuration and operating characteristics on the overall plant cycle calculations. This simplified model of the fuel cell is not intended to be a detailed authoritative representation of exact fuel cell behavior. Instead, it provides parametric interrelationships important to the overall system.

Fuel Cell Subsystem Description. The fuel cell subsystem is considered to consist of the following elements, as indicated in Figure 5-1:

- Fuel Cell: anode, cathode, electrolyte
- Adjustable anode recirculation, venting and heat rejection provision
- Catalytic combustor for anode products
- Cathode stream processing, water knockout, additional air
- Adjustable cathode recirculation, venting and heat rejection provision

The fuel cell subsystem configuration thus considered may be used for simulation of either the oil-fired or the coal-fired plant by suitable selection of parameter values for the above elements, permitting the development of a single fuel cell subsystem model.

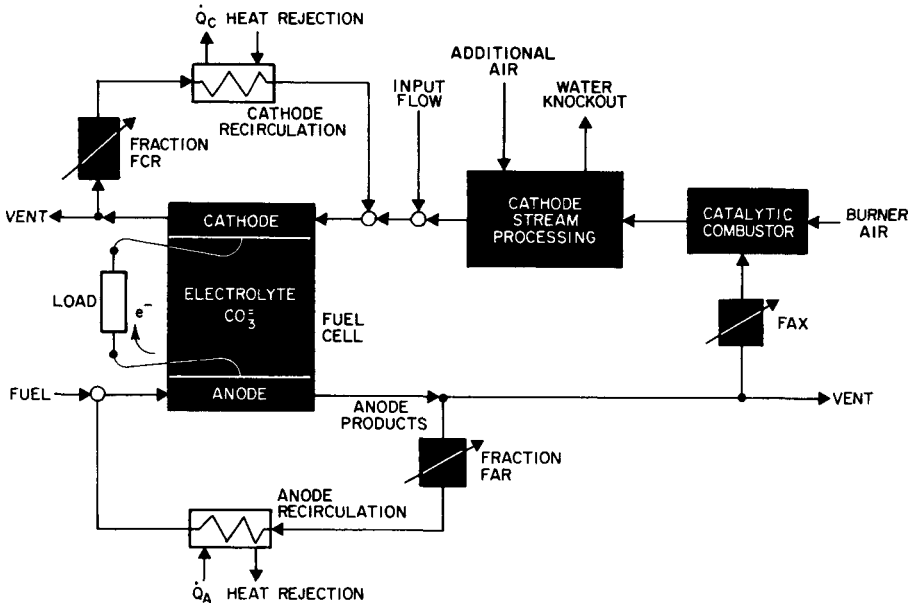

Figure 5-1. Fuel Cell Subsystem

Modeling Approach. A modular approach for the lumped parameter model has been used, based on suitable approximations to first principle relationships. Chemical equilibrium conditions, assumed for the anode and cathode reactions, are utilized along with mass balance and heat balance calculations. Throughout this subsystem, the

model computes flow rates, heat fluxes, temperatures, and gas compositions as well as the fuel cell electric performance. The fuel cell model itself represents the electrochemical reactions, including important gas shift reactions and electrochemical performance.

Assuming counterflow operation, theoretical zero-current density voltages are calculated both for the anode entry/cathode exit region and the anode exit/cathode entry region. The effective zero-current density cell voltage is then based on the calculation log mean of these potential differences. A representation of polarization loss is incorporated in a manner which permits ease of modification to represent particular cell electrolyte characteristics.

We used experimental data to quantify the polarization effects, thus permitting a gross thermal analysis to follow.

Model Description

Fuel Cell Representation. Anode. The governing electrochemical reaction for the fuel cell anode is:

$$CO_3^{=} + H_2 \longrightarrow CO_2 + H_2O + 2e^- \qquad (5\text{-}1)$$

An additional chemical reaction considered to occur at the anode is the homogeneous water gas shift reaction,

$$H_2O + CO \rightleftharpoons H_2 + CO_2 \qquad (5\text{-}2)$$

assumed to be in equilibrium at the anode at all times. This process provides additional hydrogen to the anode from the CO in the gas.

The model also includes provision for the methane steam reforming reaction. Since there is some uncertainty about methane's exact role in the process, we can choose the equation constant according to the assumed extent of the reaction,

$$CH_4 + H_2O \rightleftharpoons CO + 3H_2 \qquad (5\text{-}3)$$

The model permits methane to form, thus scavenging fuel. However, the model calculations optionally do not permit methane to reform back to fuel. Since methane is considered non-reactive in the electrochemical reactions, we treat it as an inert, along with nitrogen, in the calculation of the fuel cell performance characteristics.

In addition, the model includes oxidation reactions for the catalytic combustion of the anode products (less recycle/vent portions), as well as the removal of moisture (water knockout) from the gas upstream of the cathode. Discussions in this section provide further detail on these reactions.

The gas comprising the energy supply to the anode is considered to consist of a mixture of H_2, CO, CO_2, CH_4, H_2O and N_2. For the purposes of the study, methane can be considered an inert as far as participating in the anode electrochemical reactions. This is accomplished in the model by inhibiting the reformation of methane to carbon monoxide.

In the electrochemical reaction associated with the anode, given in Equation 5-1, carbonate ions migrate through the electrolyte from the cathode to combine with hydrogen from the fuel gas, releasing two moles of electrons at the electrode for each mole of carbonate ions.

When the gas enters the anode and encounters the nickel catalyst, but before any electrochemical action occurs, it is assumed that the homogeneous water gas shift reaction, Equation 5-2, takes place and attains equilibrium conditions. Further, the shift reaction kinetics are considered instantaneous compared to the gas residence time in the cell, and the reaction is assumed to remain in equilibrium. Then, as the gas passes across the anode electrode, the hydrogen which is consumed is partially replenished as a result of the shift reaction.

The third reaction considered for the anode is the steam reforming of methane, Equation 5-3. As discussed previously, some uncertainty exists regarding the exact involvement of methane in the reactions. In the model, inclusion of the fuel scavenging effect of methanation reaction permits us to evaluate the sensitivity of the process analysis to assumptions regarding methane behavior.

The utilization of available hydrogen by the anode reactions is defined as:

$$U_A = 1.0 - \frac{\text{Moles of } (H_2 + CO) \text{ at Anode Exit}}{\text{Moles of } (H_2 + CO) \text{ at Anode Inlet}^*} \quad (5\text{-}4)$$

This representation reflects that for each mole of CO in the fuel, one mole of H_2 will be potentially available through the shift reaction. Therefore, if the fuel flow and composition are specified and a value of anode utilization assumed, the rate of hydrogen consumption in the anode electrochemical reaction is defined, leading to the associated carbonate ion flow rate and the number of electrons released, from Equation 5-1.

An additional calculation examines the equilibration at the anode inlet point to determine whether the relationship between the gas constituents threatens carbon deposition in the fuel cell anode, comparing the ratio of partial pressures with the equilibrium constant for the reaction.

$$CO_2 + 2H_2 = C + 2H_2O \quad (5\text{-}5)$$

Cathode Reaction. Receiving electrons from the load, the cathode reaction utilizes oxygen and carbon dioxide from the cathode inlet stream to provide the electrolyte with the carbonate ions needed for the anode reaction.

$$CO_2 + 1/2\ O_2 + 2e^- = CO_3^= \quad (5\text{-}6)$$

For each mole of carbonate ions released, the reaction requires two moles of electrons, one mole of carbon dioxide and one-half mole of oxygen.

Overall Cell Reaction and Polarization Effects. The overall cell reaction, considering the anode and cathode reactions (Equations 5-1 and 5-5) is:

$$2H_2 + O_2 = 2H_2O \quad (5\text{-}7)$$

The Nernst voltage, or reversible cell potential, is:

$$V = V_o - \frac{RT}{nF} \ln Q' \quad (5\text{-}8)$$

*Prior to equilibration

where the standard cell potential (at 298 K and 1 atm) is:

$$V_o = - \frac{G^o}{nF} \qquad (5\text{-}9)$$

The ratio of chemical activities, Q', is considered the calculated equilibrium constant associated with the overall cell reaction:

$$K_p = \frac{\left[H_2O\right]_A^2 \left[CO_2\right]_A^2}{\left[H_2\right]_A^2 \left[O_2\right]_C \left[CO_2\right]_C^2} \qquad (5\text{-}10)$$

Where the subscripts A and C refer, respectively, to the constituent partial pressures at the anode and cathode.

Based on an assumed counterflow cell arrangement, Equations 5-7, 5-8, 5-9 are used to calculate the theoretical zero current density, or reversible voltages at the anode entry/cathode exit and the anode exit/cathode entry. The effective reversible cell potential is then based on the calculated log mean of these potential differences.

The fuel cell terminal voltage is the reversible cell potential minus the internal voltage drop (polarization). For the molten carbonate fuel cell model, the polarization is considered to appear exclusively as a resistive effect, proportional to the value of current density. Experimental evidence supports this treatment of the polarization effect. The cell terminal voltage then is:

$$V_T = V - JR_p \qquad (5\text{-}11)$$

where J is the current density (A/cm^2) and R_p is the polarization resistance ($\Omega\ cm^2$). The value of polarization resistance used in the model calculations is 0.7 $\Omega\ cm^2$, based on state-of-the-art performance for molten carbonate fuel cells projected for 1990. Fuel Cell Analytical Model Performance Evaluation discusses this further.

Thermal Balance. The thermal balance of the cell reflects that the chemical energy released by the reaction of gas constituents at the anode and cathode appears as the sum of the electrical energy delivered to the load plus the increase of sensible heat of the gas streams passing through the cell.

The total (chemical) enthalpy of each gas constituent, a function of temperature, consists of its sensible heat plus heat of formation. The model calculates the total chemical energy entering the cell as the sum of the products of total enthalpy and flow of the anode inlet and cathode inlet streams. Similarly, the model calculates the total chemical energy of the streams leaving the cell. The difference between these values represents the electrical energy delivered to the load.

In addition the model postulates that the temperatures of the gas streams leaving the cell are equal to each other, and in a fixed relationship to the defined cell operating temperature, because of the flow rates, areas and heat transfer characteristics involved. For any given incoming gas temperature at the anode, the model determines the temperature of the gas entering the cathode to effect a thermal balance for a given operating condition.

Anode Recirculation Loop. The model includes provision for the anode recirculation loop, indicated in Figure 5-1, which affects both the electrochemical and thermal balance calculations. A defined fraction of the flow of the anode exit gas is added to the incoming fuel to establish the anode inlet gas. The resultant mixture is then considered to equilibrate at the anode inlet (at the temperature of the fuel cell), as discussed in Fuel Cell Representation. Anode. Solution of the mass balance equations utilizes an iterative approach, first assuming no recirculation. In the thermal balance calculations, the model determines the heat rejection required to cool the gas in the anode recirculation path.

Cathode Recirculation Loop. Further, the model also includes a provision to recirculate a portion of the cathode exhaust stream to the cathode inlet. Both the cathode mass balance and thermal balance calculations are affected by the defined magnitude of the cathode recirculation fraction. For a defined fraction of the cathode products to be recirculated to the cathode inlet, there is a closed solution to the mass balance calculations around the cathode.

Because the amount of recirculation flow influences the gas flow through the cathode, as well as the concentration of the constitutents, the model calculations provide a convenient means of evaluating the effectiveness of cathode recirculation flow adjustments to assist in thermal control of the fuel cell subsystem.

Catalytic Combustor. Mass Balance. The constituents of the anode products include unreacted fuel components. These are considered to react completely by oxidation in the catalytic combustor.

$$2H_2 + O_2 = 2H_2O \quad (5\text{-}12)$$

$$2CO + O_2 = 2CO_2 \quad (5\text{-}13)$$

$$CH_4 + 2O_2 = CO_2 + 2H_2O \quad (5\text{-}14)$$

By considering the fraction of anode products introduced to the catalytic combustor, along with the amount of air, a mass balance calculation results in the flow and chemical constituents of the combustor exhaust stream.

Thermal Balance. A thermal balance model approach similar to that described above in Fuel Cell Representation. Anode permits determination of the temperature and enthalpy of the product stream from the catalytic combustor. The total (chemical) enthalpy of each of the gas constituents is determined by the stored thermodynamic characteristics provided in the model.

Cathode Stream (Burner Products) Processing. To provide for flexibility in using the model for evaluating a number of system configurations, the modular nature of the simulation permits further processing of the gas stream ahead of the cathode. Two examples are the provision for moisture removal (water knockout) and the introduction of additional air beyond that required by the catalytic combustor, affecting both mass balance and thermal balance calculations.

Simulation Implementation Approach. Mass Balance. The procedure for determining predicted cell performance by the digital computer simulation program is discussed briefly. The modular configuration of the simulation model is indicated in Figure 5-2. Cell operating temperature and pressure are defined. Anode conditions specified by the user include modal concentrations of the fuel constituents CO, H_2, H_2O, CO_2, CH_4 and N_2, as well as the fuel flow in moles per second (a value of 1.0 will normalize calculations on a per mole of fuel per second basis). Also specified is the anode utilization and the fraction of the anode products recirculated back to the anode inlet to mix with the incoming fuel flow, if desired. The anode calculations proceed on an iterative basis, first assuming no recirculation. Equilibrium calculations are made for the anode inlet, including no reaction with the carbonate ions, to equilibrate elsewhere, the water gas shift reaction and the optional methane reaction (as discussed in Fuel Cell Representation. Anode). Based on work by Gumz, one uses polynomial expressions to define the equilibrium constants as a function of temperature (degrees kelvin):

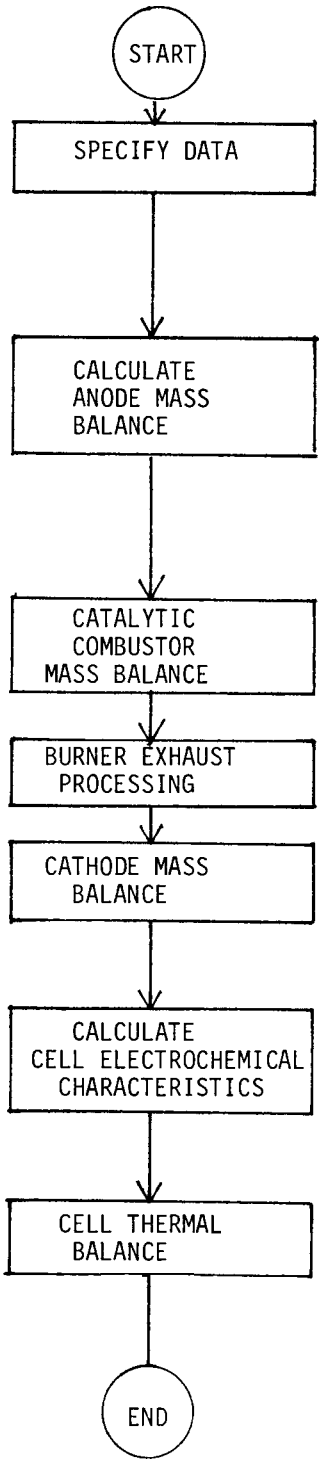

- Fuel Composition
- Pressure, Temperatures
- Recirculation Fractions
- Cell Characteristics
- Gas Flows, Anode (Hydrogen) Utilization
- Etc.

Iterative loop, initially assume anode inlet concentrations same as fuel; will change during subsequent calculations with anode recirculation mixing.
Determine resultant concentrations and flow rates at anode entry and exit. Determine carbonate ion flow.

Determine flow rate and composition of gas at exit of catalytic combustor.

Determine mass balance effect of additional air and/or moisture removal, if included.

Based on incoming gas flow, composition, carbonate ion flow and recirculation fraction, calculate gas flow rate and composition at cathode inlet and exit.

Based on calculated flow rates and gas compositions, calculate Nernst voltages at fuel cell boundaries and the average value. Calculate terminal voltage as a function of current density.

Based on thermodynamic data for gas constituents and flow rates, calculate cathode inlet gas temperature required for balance, and associated heat rejection magnitude as a function of current density.

Figure 5-2. **Fuel Cell Model Approach**

$$\log_{10}(K_W) = 36.72508 - 3994.704/T + 4.462408E\text{-}3(T) - 0.67184\ E\text{-}6(T^2) - 12.22028\ \log_{10}T \quad (5\text{-}15)$$

$$\log_{10}(K_W) = -20.39417 - 9488.79/T - 3.5752\ E\text{-}3(T) + 0.439348\ E\text{-}6(T^2) + 11.48142\ \log_{10}T \quad (5\text{-}16)$$

where K_W applies to the water gas shift reaction (Equation 2) and K_M applies to steam reforming of methane (Equation 3).

Next, the equilibrium mass balance conditions at the anode exit are calculated, considering the addition of carbon and oxygen atoms from the carbonate ions in the electrolyte. Again the water gas shift and methane reactions (as noted) are considered in equilibrium. If there is no anode recirculation, this completes the mass balance calculations for the anode.

If there is anode recirculation, the calculation procedure described in the preceding is repeated iteratively, with the flow and composition of the stream entering the anode inlet being a calculated mixture of the fuel and a portion of the anode products calculated in the preceding iteration. The convergence is rapid, resulting in calculated flow rates and compositions at the anode entry and exit.

A mass balance calculation is made to determine the flow and composition of the products from the catalytic combustor. For the computer simulation, the user specifies the fraction of the products from the anode (less recirculation) which goes to the combustor as well as the burner air flow rate.

Provision exists for further calculations in the Burner Products Processing module, to include considerations such as water knockout and the introduction of additional air. Additionally, options can be exercised by utilizing the Cathode Test Input feature; this provides a means of introducing a defined flow (rate and composition) to the cathode system by means of the cathode test input. For example, sensitivity studies can be made under controlled cathode conditions by specifying the test input and setting the burner air flow and the anode exit flow fraction (FAX) to zero. This input can also be utilized to introduce additional air or to simulate water removal from the stream (by using a negative H_2O rate). The resultant flow to the cathode system is calculated as the sum of the burner products processing module and the cathode test input.

The simulation of the cathode system is similar to, but somewhat simpler than, the anode system calculation. With the cathode recirculation fraction, FCR, defined by the user and calculated values available for the cathode system input flow and carbonate ion participation, one can directly calculate all the cathode flow rates and compositions. Iteration is not required because of the absence of shift reactions. The resulting calculated constituent modal concentrations at the cathode inlet and outlet are then used in the electrochemical calculations to determine the cell operating voltage.

Thermal Balance. The fuel cell electrochemical performance is closely related to the cell heat balance considerations. The calculations described in the preceding were based on the gas temperatures in the fuel cell being defined by the user; it is assumed that both anode and cathode exit are at the same temperature. This assumption is based on the residence time of the gas traversing the cell and the surface area to which it is exposed. The data specified for the model calculation include values for the operating temperature of the cell.

Further, it is assumed that sufficient heat rejection capacity exists in the anode recirculation path to cool the recirculated products as required. The energy balance calculation considers the energy released by the chemical reactions, based on changes in total enthalpy (sensible enthalpy plus heat of formation). For the given recirculation rate, the simulation calculates the cathode heat rejection rate and resultant gas temperature into the cathode which are required for the overall cell heat balance. These results may be examined for reasonableness of temperature and heat rejection values for the given recirculation rate.

Cell Performance Calculations. The predicted performance of the cell, calculated by the model for several values of current density, includes parameters such as terminal voltage, electrical power efficiency (power/HHV fuel) and associated fuel flow density (mole/sec cm^2). Also included, are various calculated heat balance parameters. Results based on simulation runs are discussed further in Model Results.

Model Results

The fuel cell model has been used to explore the relationships between various fuel cell subsystem parameters such as efficiency, power density, anode recycle, utilization, compositions, etc. These relationships are complex and multidimensional, and a rigorous treatment is not appropriate in this report. Therefore, to serve

illustrations of the power of such a model, and to demonstrate the type of study that is being conducted, three parametric curves are shown.

Figure 5-3 shows the calculated fuel cell voltage as a function of current density for constant inlet gas compositions and a constant anode utilization of 73.9%. Note that the gas compositions shown are those of Case 1 Coal-Fired Plant described in Section 3.

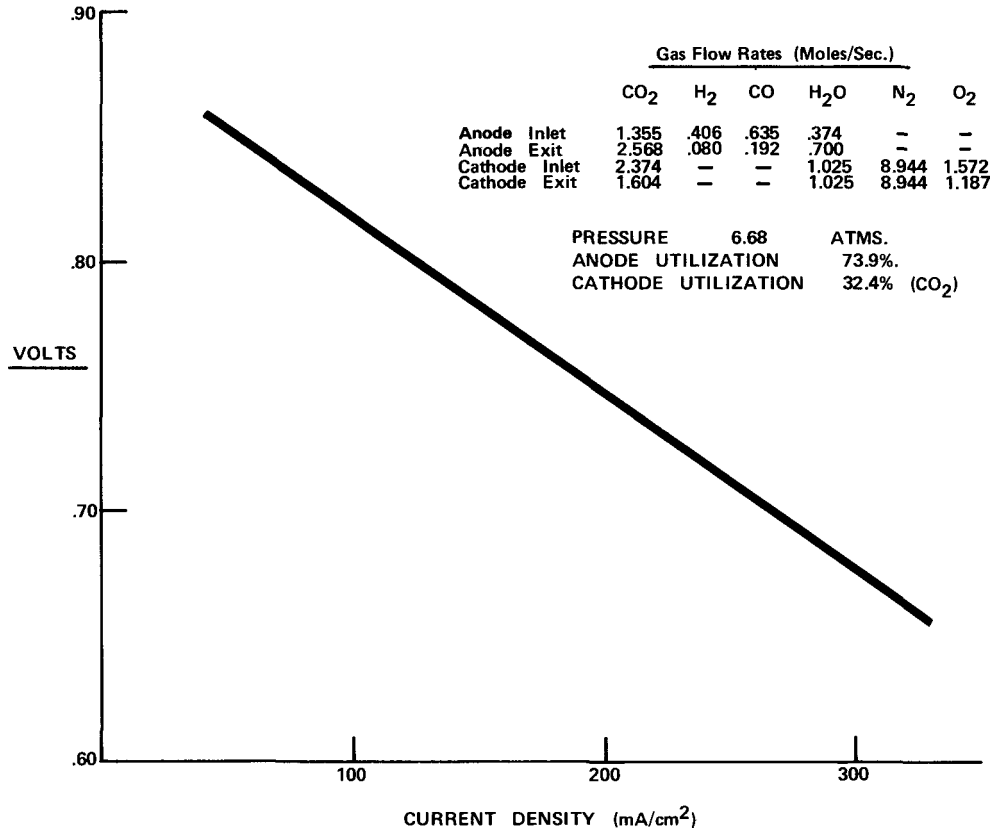

Figure 5-3. Cell Voltage versus Current Density (Methane Assumed Not to Form)

One may observe that for lower current densities, the voltage is greater because of fewer polarization losses. This is illustrated by Figure 5-4, in which cell

power density is plotted as a function of cell efficiency, where power density and cell efficiency is defined as:

$$\text{Power Density} = (\text{Cell voltage} \times \text{cell current density})$$

$$\text{Cell Efficiency} = \frac{(\text{Cell power density})}{(\text{Anode inlet gas HHV}) \times (\text{Anode flow rate/cm}^2)}$$

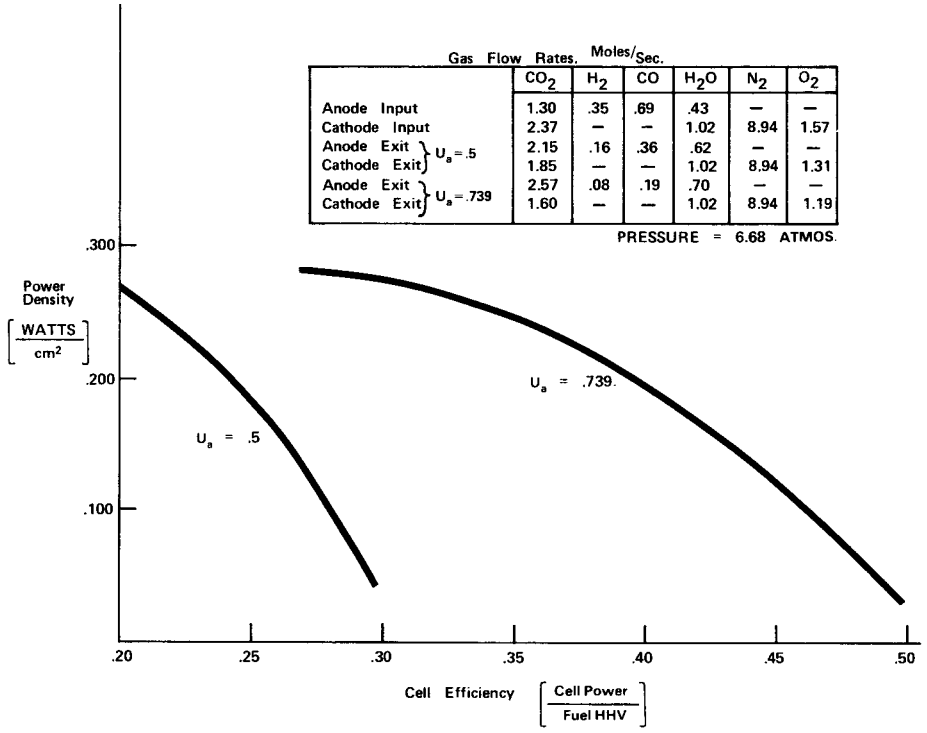

	CO_2	H_2	CO	H_2O	N_2	O_2
Anode Input	1.30	.35	.69	.43	—	—
Cathode Input	2.37	—	—	1.02	8.94	1.57
Anode Exit (U_a=.5)	2.15	.16	.36	.62	—	—
Cathode Exit (U_a=.5)	1.85	—	—	1.02	8.94	1.31
Anode Exit (U_a=.739)	2.57	.08	.19	.70	—	—
Cathode Exit (U_a=.739)	1.60	—	—	1.02	8.94	1.19

Figure 5-4. Power Density versus Cell Efficiency for Two Values of Anode Utilization (Methane Assumed Not to Form)

This is shown for two different values of anode utilization (73.9% and 50%). Curves of this type are vital to the completion of a meaningful plant design optimization and selection. This figure, for example, aids in the evaluation of the impact of fuel cell capital cost changes (inversely proportional to power density) on the fuel cell operating cost (inversely proportional to cell efficiency).

Among the major design constraints, carbon formation in the anode inlet plays a most significant role in cell operating condition selection. Achievement of a carbon-free anode inlet composition is generally through the use of anode gas re-

cycle. Figure 5-5 shows the results of one such study. In this figure, a constant fuel gas source (composition and flow rate) is assumed, and percentage recirculation of the anode exit gases is varied; anode utilization is varied correspondingly to maintain constant exit composition. Cathode inlet flow rates are held fixed. It will be observed that increasing recirculation does in fact produce a carbon-free condition, but that for a selected current density, the cell efficiency is reduced.

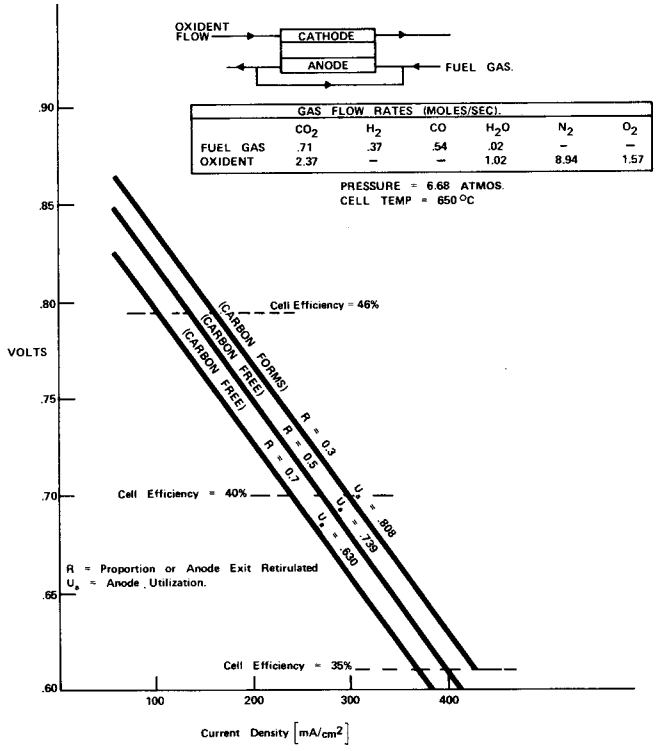

Figure 5-5. Effect of Anode Recirculation on Cell Performance

Fuel Cell Analytical Model Performance Evaluation

We evaluated the fuel cell analytical model to determine its ability to predict fuel cell performance by comparing the computer model results with experimental data obtained at the Institute of Gas Technology (IGT) and at General Electric (GE). The specific objective of this evaluation was to verify that the fuel cell model would accurately calculate the reversible cell potential (at zero current density) and the losses for each of the cases considered. This section discusses the methods and results of this analysis.

When current is drawn from the cell, the voltage is always less than the thermodynamic maximum for a practical fuel cell because of irreversible effects that occur within the cell. The current density-voltage curve (or polarization curve) is probably the most important single index of fuel cell performance. However, the curve is unique to an individual cell (or stack of cells) and represents only one set of operating conditions, such as pressure temperature, fuel gas composition and utilization. For each set of operating conditions there is a separate polarization curve so that an individual fuel cell is in reality characterized by a family of current density-voltage curves covering all operating conditions. The situation is further complicated, however, since fuel cell performance is often not invariant with time. At the beginning of cell operation, cell performance frequently improves with time as cell components "break in," whereas later in its life cell performance declines because its components degrade. Thus, any discussion of cell performance should also include its time in life.

The above discussion points out the problems involved with developing a rigorous analytical model of a fuel cell. Therefore, the molten carbonate fuel cell computer model contains approximations and simplifications which can be replaced with more precise relationships, based on experimental data, as they become available. For the present, we compared the first-generation analytical model with available experimental data to evaluate its prediction of fuel cell performance.

The experimental fuel cell data came from two sources: IGT under contract to Argonne National Laboratory (1); and GE under contract to the Department of Energy (2). The chosen data runs were intended to be representative of as wide a range of operating conditions as possible, consistent with the capabilities of the analytical model and with established design specifications of the molten carbonate fuel cell. Thus, all data runs chosen for comparative purposes were at 650 ^{o}C but with varying fuel gas composition, flow rates and fuel utilizations. Also, since the model does not have the ability to account for changes in cell performance as a function of life, all of the runs selected were close to the optimum cell performance (after the initial "break-in" period but before significant degradation effects were evident).

There were a total of nine runs, three from GE and six from IGT, as shown in Table 5-1. The three GE runs were from DECP Run No. 005 (after 312 hours of cell operation) at three different fuel gas compositions. The anode gas flow rate was held constant at 440 cc/min and the cathode gas flow rate at 370 cc/min for each

Table 5-1

PREDICTED VERSUS EXPERIMENTAL CELL VOLTAGE - DATA SOURCE

Data Point Identification	Voltage at Zero Current Density		Anode Gas Flow Rates (Mol/Sec)						Cathode Gas Flow Rates (Mol/Sec)				Anode Fuel* Utilization	Cathode** Utilization
	Experimental	Calculated	CO_2	CO	H_2	N_2	H_2O	CH_4	O_2	N_2	CO_2	H_2O		
DECP A	1.047	1.052	0.223	0.0	0.374	0.403	0.0	0.0	0.152	0.563	0.285	0.0	0.0	0.0
DECP B	1.075	1.082	0.243	0.0	0.754	0.0	0.0	0.003	0.152	0.563	0.285	0.0	0.0	0.0
DECP C	1.108	1.132	0.243	0.0	0.754	0.0	0.0	0.003	0.333	0.0	0.667	0.0	0.0	0.0
IGT 1	0.942	0.989	0.081	0.196	0.160	0.499	0.034	0.030	0.247	0.908	0.495	0.051	71.0	51.3
IGT 2	0.943	0.966	0.158	0.375	0.365	0.007	0.078	0.017	0.522	1.922	1.048	0.108	71.0	50.3
IGT 3	0.964	0.976	0.074	0.100	0.600	0.0	0.226	0.0	0.479	1.762	0.960	0.099	69.0	50.5
IGT 4	0.927	0.995	0.083	0.391	0.452	0.023	0.049	0.002	0.580	2.136	1.164	0.120	70.0	50.9
IGT 5	1.010	1.060	0.083	0.391	0.452	0.023	0.049	0.002	0.334	1.228	0.669	0.069	20.0	25.3
IGT 6	1.002	1.039	0.083	0.391	0.452	0.023	0.049	0.002	0.116	0.427	0.233	0.024	20.0	72.7

NOTES: All Above Cells for 650 ^{o}C Operating Temperature.
*Anode Fuel Utilization - Mole % of ($CO+H_2$) Consumed.
**Cathode Utilization = Mole% of Oxygen Consumed.

of the runs. Because the fuel gas flows were constant, the fuel utilization varied with the current density. The zero current density cell potential was determined for each run by extrapolarization and calculation of the respective polarization curve; this is the value shown on Table 5-1.

For the GE runs, the fuel utilization was zero at zero current density since no power was being generated. This is also indicated on Table 5-1, as well as the gas composition for each of the runs.

The six IGT runs were performed at times of 314, 122, 172, 288, 339 and 337 hours respectively. At least four of the runs (IGT 1, 4, 5 and 6) were conducted using the same fuel cell but there was insufficient documentation in the IGT report to determine what cells were used for the other two runs. As with the GE data, the polarization curves were extrapolated to zero current density to obtain the zero current density cell potential for each run.

The appropriate data for each run was then input to the fuel cell computer model and the zero current density cell voltage calculated. For the GE data this required constructing a current density-voltage curve by inputting several values of anode utilization at the constant gas flow rate and extrapolating this curve to zero current density. For the IGT data, we required only one computer run to generate the current density-voltage curve for each data run because the anode and cathode utilizations were constant within each data run.

The zero current density cell potential predicted by the fuel cell program for each run is shown as Predicted on Table 5-1. Figure 5-6 is a plot of Predicted versus Experimental for all nine runs considered.

As can be observed from study of Figure 5-6, while the gradient appears to be an adequate match, the predicted voltages in general are lower than the experimental results. Several factors are believed to contribute to this, including

- limited data base
- model assumes zero reformation of methane
- model considers a uniform single node, countercurrent flow configuration

One should note that IGT and this report define the anode fuel utilization differently. The IGT defines fuel utilization as the hydrogen that the cell consumes electrochemically plus the hydrogen consumed or liberated by the water gas shift

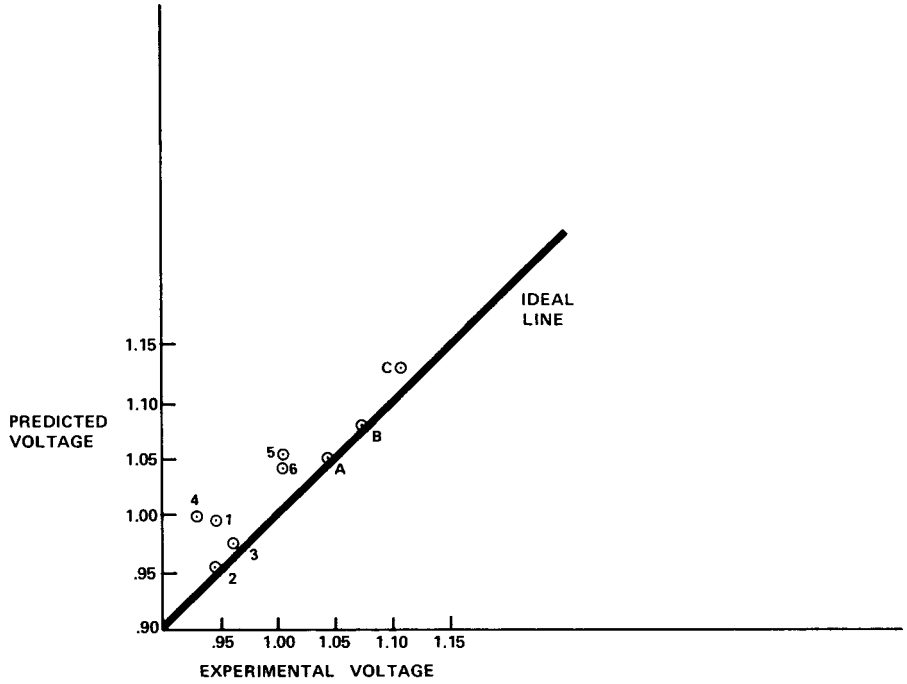

Figure 5-6. Comparison of Fuel Cell Model with Data Predicted Voltage versus Actual Voltage (At Zero Current Density)

reaction with respect to the hydrogen content of the inlet fuel gas. This definition is awkward for use in predictive studies since it requires knowing the anode outlet gas composition in order to calculate the amount of hydrogen consumed in the fuel cell, and thus involves an iterative process. The GE computer model, on the other hand, defines the anode utilization as the percent of hydrogen consumed electrochemically in the fuel cell relative to total amount of hydrogen plus carbon monoxide in the inlet fuel gas prior to equilibration. This definition is based on the assumption that all the carbon monoxide could be converted to hydrogen via the water-gas shift reaction. Thus, this definition is simply the amount of hydrogen consumed relative to the maximum theoretical hydrogen content of the fuel. The two definitions result in fuel utilizations that differ by as much as 10%. Therefore, the IGT-defined utilizations have been changed to match those used in the computer model.

The analytical model shows polarization losses as linear, so that the current density-voltage curve is a straight line, and the slope of the line ($\Omega\,cm^2$) is an input data parameter to the code. For the data runs considered, the use of a linear current density-voltage curve is found to be a good assumption, indicating that ohmic polarization is the predominant loss for these cases.

The slope of the current density-voltage curve was set at $0.7\,\Omega cm^2$ in the model. This value corresponds to the fuel cell design assumption (i.e., fuel cell performance) for the year 1990 as established in the molten carobonate fuel cell ECAS Report (Reference 3 in Section 4).

Note that for the nine experimental runs evaluated in the present study, the average slope was $1.582\,\Omega cm^2$. Therefore, the average performance of these fuel cells was markedly less than the 1990 ECAS design assumptions.

Although the fuel cell analytical model appears to predict experimental data with a reasonable degree of accuracy, we recognize that the model requires refinements, including establishment of a better representation of polarizaiton. It seems that some variation of polarization losses with fuel utilization is appropriate.

CHEMICAL EQUILIBRIUM ANALYSIS

In order to conduct meaningful, integrated, power plant cycle development studies, it is evident that chemical equilibrium analysis capability is essential. Such capability provides the method which can explore several component performances when incomplete data bases exist. In addition, such analysis will permit the assessment of the proximity of a given operating condition to a particular undesired situation (the formation of carbon). In using such analyses, however, one must give continuous and careful consideration to the realiities of equipment operation which may not be reflected in the particular model.

The areas in the plant cycle evaluation studies to which we have successfully applied chemical equilibrium-type analyses are as follows:

- Texaco gasifier (air-blown).
- Oil reformer.
- Carbon formation in fuel cell.
- Methane formation impact on fuel cell.

The adopted approach for the first two of these analyses is best described as data base extrapolation, as opposed to a mechanistic model involving detailed phenomenametric representations.

Two different chemical analysis capabilities have been established. The first is a comprehensive equilibrium calculation involving use of the JANAF tables, which

can calculate an equilibrium heat, mass and atomic balance involving many hundreds of gaseous species in the intial or product mixture. Certain solid and liquid species are also incorporated. This was used for the gasifier and reformer models. The second is a limited species capability in which the initial and product mixtures are supposed to comprise a few species only. Of these species, one is solid carbon and one is a general inerts category. This latter capability, while not so comprehensive, is economical in use, and thus is particularly useful both for inclusion as part of other models such as the fuel cell, and for general scoping study purposes.

We will describe each of these capabilities and then discuss the extension of this capability to represent the Texaco gasifier and the autothermal reformer.

Chemical Equilibrium Subroutine Package

CESP (Chemical Equilibrium Subroutine Package) is a group of Fortran IV subroutines which calculate high-temperature chemical equilibria. The subroutines are based on those in a Propellant Evaluation Computer Program at the Naval Ordnance Test Station. The basic methods in that program for determining equilibrium have been adopted and are described in References 4 and 5. Modifications by GE have improved the Fortran logic and simplified its use for power plant related evaluations.

Product chemical composition is evaluated using as input data, the weight proportions of the elements in the system, and two mixture properties (e.g. pressure and temperature). All possible reaction products, including those of dissociation and ionization, are read from a magnetic tape, which contains JANAF data (see Reference 6) on their thermodynamic properties for 298 and 6000 K. Based on the product species properties, the CESP program then seeks a product mixture which satisfies energy, mass and atomic balance. The method of solution is the classical technique of Gibbs free energy minimization. The properties of the mixture, such as temperature entropy and enthalpy, are also calculated. Figure 5-7 shows a sample calculation result.

Limited Species Equilibrium Model

The analytical tool was developed to provide a convenient means of calculating chemical equilibrium conditions and to determine the carbon deposition tendency of the resultant gas mixture. The species considered are: C, CO_2, N_2, O_2, H_2O, H_2 and CH_4. The time-sharing computer program assumes there is insufficient oxygen

for complete conversion, with a reducing condition existing in the resultant gas mixture.

Two reactions assumed to be in equilibrium are the homogeneous water-gas shift reaction and the steam reforming of methane.

LINE NO. (INPUT DATA)

100	Identification, Number of Components
110-140	Component Description and Atomic Composition
150	Guess at Equilibrium Temperature (to speed iteration)
160	Numbers of Inputs
170	Preheat Temperature
180-210	Heat of Formation
220	Pressure
230	Equivalence Ratio, Percent of Each Component

```
100                          ESPD    4
110 FLUOR COAL--O2 BLOWN              4862C 4436H  526O   75N  101S
120 WATER AT  140 F                   2000H 10000
130 STEAM AT AIR PREHEAT TEMP         2000H 10000
140 AIR                               98240  151N   24AR
150   1644.26
160         4          1          1          1
170    300.00
180   -391.88
190  -3759.46
200  -3489.41
210     29.67
220     40.82
230      2.71      42.06      21.16       0.       36.79
```

MOLE FRACTIONS OF PRODUCTS

CO	0.4352/4.35E-01	H2	0.3226/3.23E-01	H2O	0.1224/1.22E-01
CO2	0.0894/8.94E-02	H2S	0.0107/1.07E-02	CH4	0.0105/1.05E-02
N2	0.0075/7.52E-03	AR	0.0011/1.09E-03	COS	0.0005/4.69E-04
NH3	0.0001/7.53E-05	CNH	0.0000/6.86E-06	CH2O	0.0000/5.36E-06
HS	0.0000/3.54E-06	CS2	0.0000/5.51E-07	CS	0.0000/4.39E-07
S2	0.0000/2.58E-07	H	0.0000/1.33E-07	C2H2	0.0000/3.86E-08
SO2	0.0000/5.54E-09	SO	0.0000/1.29E-09	HO	0.0000/7.07E-10
S	0.0000/2.56E-10	S2O	0.0000/1.18E-10	NS	0.0000/2.74E-12
NO	0.0000/7.53E-13	NH	0.0000/2.10E-14	NHO	0.0000/9.16E-16
O	0.0000/2.79E-16	O2	0.0000/5.17E-17	N	0.0000/4.34E-18

		AIR PREHEAT TEMPERATURE (DEG F)
ER	P(ATM)	300.
2.7100	40.8	1916.

Figure 5-7. Sample CESP Run.

$$H_2O + CO \rightarrow H_2 + CO_2$$

$$CH_4 + H_2O \rightleftarrows CO + 3H_2$$

Using a combination of mass balance equations for each specie and the equilibrium equations for the two reactions, the program calculates the product constituents.

A check is then made on the equilibrium of the reaction for the formation of carbon:

$$CO_2 + 2H_2 \rightleftarrows C + 2H_2O$$

If the equilibrium gaseous concentrations are consistent with carbon formation we assume an amount of carbon and repeat iteratively the equilibrium calculations until all relationships are satisfied. The results of the calculations, then, include the amounts of carbon (if any) and the other constituent species.

For example, Figure 5-8 indicates the theoretical impact of temperature and H_2O concentration upon potential carbon formation for the fuel composition of the reference oxygen-blown case. For a given composition, a temperature increase of the mixture reduces the tendency of carbon to form if equilibration occurs. Likewise, for a given temperature, an increase of the H_2O concentration also decreases the tendency for carbon to form. You will note that this tendency is one of the significant potential benefits of anode recirculation for the fuel cell subsystem.

The results of the limited species model compare very closely with the more complete CESP for the identified species. The limited species equilibrium model has been used to investigate conditions at various points in the cycle and is incorporated as a subset of the fuel cell model.

AIR-BLOWN GASIFIER (TEXACO) MODEL

Reference (7) gives performance information for the air-blown Texaco gasifier at two different air preheat temperatures. Early scoping studies showed this preheat temperature to be an important parameter, and thus a model was generated to provide an extension to this limited data base.

The feed conditions for the 1500 ^{o}F air preheat case were equilibrated by use of a modified version of the CESP program described earlier in the section "Chemical

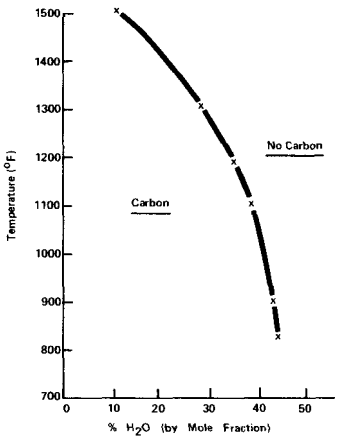

Figure 5-8. Theoretical Boundary for Carbon Formation for Reference Fuel

Equilibrium Subroutine Package." An allowance was made for heat loss and the thermal sink effect of the ash in the coal; the ash was assumed chemically inert. We then compared the results with the Texaco performance information, as shown in Table 5-2.

From this comparison, one may draw the following conclusions:

- The water-gas shift reaction is not in equilibrium at the final temperature in the Texaco case.
- Methane formation is not in equilibrium in the Texaco case, but is small enough to ignore.
- The total number of moles is a good match.
- The sum of the moles of H_2, H_2O, CO and CO_2 is a good match.

Based on this, a postprocessor was applied to the CESP generated data, which shifted the water-gas reaction components into equilibrium at a lower temperature. We assumed this lower temperature (2150 ^{o}F) to be in a fixed ratio to the computed equilibrium temperature. Suitable correction was made in the final temperature to allow for the net enthalpy change of the water-gas reaction shift.

It is to be expected that the match at 1500 ^{o}F air preheat shown in Table 5-2 is good since that was the data base used; however, Table 5-4 shows that match to be equally good for the 600 ^{o}F preheat case.

Table 5-2

COMPARISON OF EQUILIBRIUM
CALCULATION VERSUS TEXACO DATA

Input Data

Coal	162,315 #/hr
Water (at 300 ^{o}F)	117,527 #/hr
Air (at 1500 ^{o}F)	734,391 #/hr
Pressure	600 psig

Product Gases	CESP (Equilibrium)	Texaco
CO	16.55	15.85
H_2	11.02	11.59
CO_2	6.98	7.73
H_2O	15.21	14.08
CH_4	0.00	0.02
AR	0.50	0.63
N_2	49.24	49.61
H_2S	0.46	0.46
COS	0.02	0.03
Temperature	2539. ^{o}F	2500. ^{o}F

Figures 5-9, 5-10, and 5-11 show the use of this model to explore variation in operating conditions about a 1040 ^{o}F preheat point. One may note that the air/coal feed ratio has a marked effect on Heating Value Ratio $= \frac{\text{HHV of } (H_2+CO)}{\text{HHV of coal}}$, where air preheat temperature and water/coal ratio have only a slight effect. Directions for possible optimization studies are clearly indicated.

AUTOTHERMAL REFORMER

Reference (8) shows autothermal performance for #2 fuel oil. This source and others indicate that one may consider the device an equilibrium device after making suitable allowance for heat loss and ash content. Table 5-5 shows a comparison with a suitably modified CESP equilibrium calculation and the information referenced above.

Table 5-3

COMPARISON OF TEXACO GASIFIER MODEL
(1500 ^{o}F air preheat)

Product Gases	Model	Texaco
CO	15.78	15.85
H_2	11.79	11.59
CO_2	7.75	7.73
H_2O	14.44	14.08
CH_4	0.00	0.02
A_R	0.50	0.63
N_2	49.24	49.61
H_2S	0.46	0.46
COS	0.02	0.03
Temperature	2544 ^{o}F	2500 ^{o}F

Input	
Coal	162,315 #/hr
Water (at 300 ^{o}F)	117,527 #/hr
Air (at 1500 ^{o}F)	734,391 #/hr
Pressure	600 psig

This model will therefore be used as a representation of the autothermal reformer. However, we must emphasize that the model, at this time, only considers true equilibrium, and in the case of carbon formation, this is somewhat misleading. As discussed in Section 4, the real carbon formation limit of the reformer is very restrictive in terms of possible operating conditions. Since the direction of carbon formation is also the direction of improved theoretical performance, the thrust of future hardware development is clear.

Table 5-4

COMPARISON OF TEXACO GASIFIER MODEL
(600 °F air pre-heat)

Product Gases	Model	Texaco
CO	12.47	12.75
H_2	8.99	8.85
CO_2	9.27	9.04
H_2O	15.33	15.14
CH_4	0.00	0.02
A_R	0.54	0.43
N_2	52.94	53.33
H_2S	0.42	0.43
COS	0.02	0.03
Temperature	2446 °F	2450 °F
Input		
Coal	193,029 #/hr	
Water (300 °F)	139,765 #/hr	
Air (600 °F)	1,016,437 #/hr	
Pressure	600 psig	

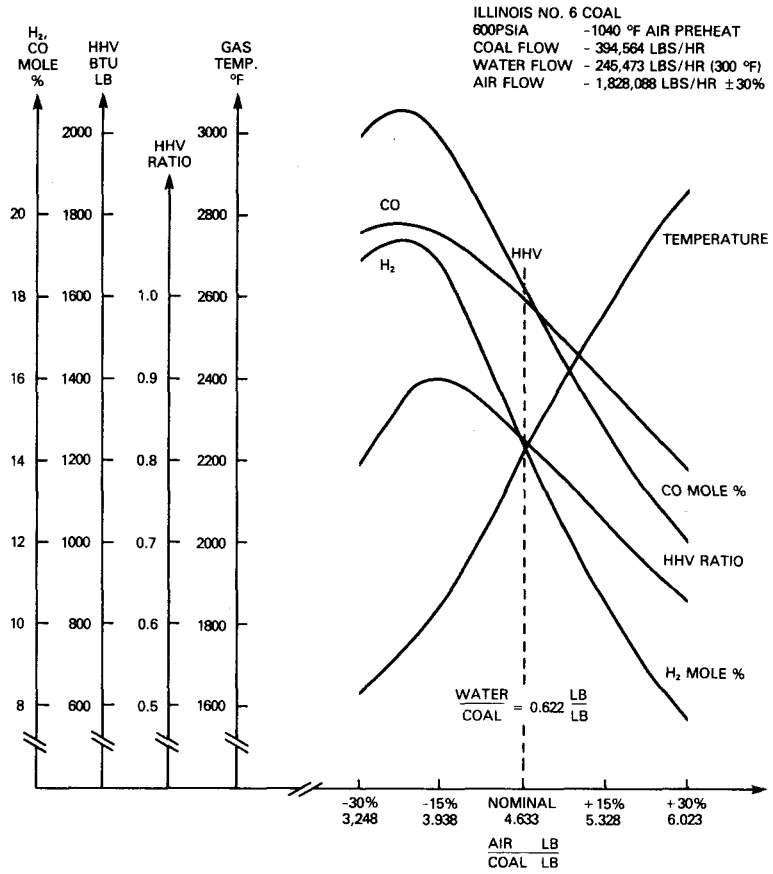

Figure 5-9. Gasifier Variation of Air/Coal

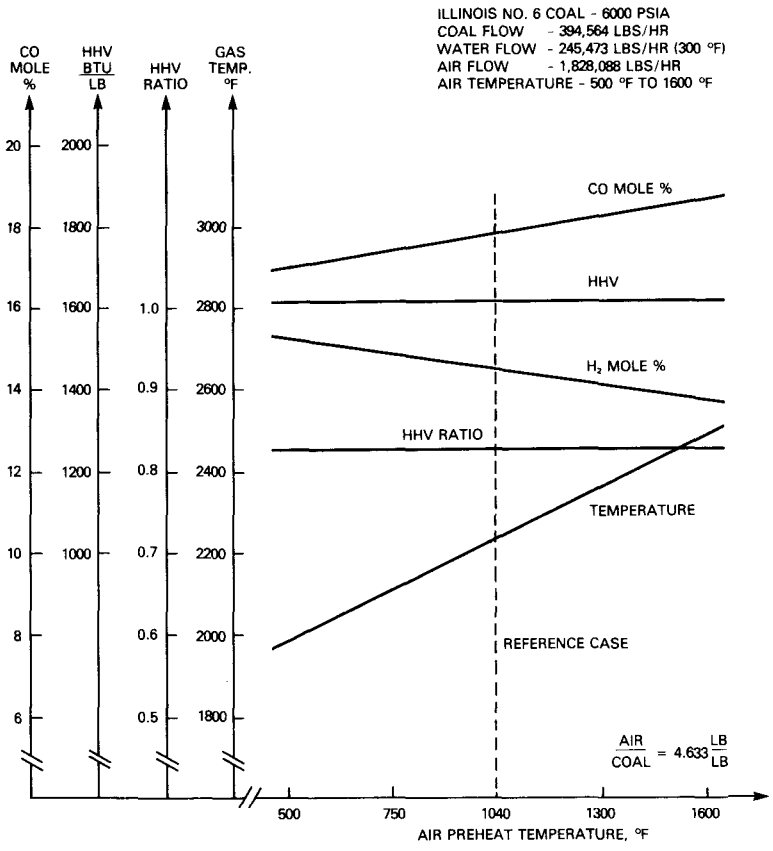

Figure 5-10. Gasifier Variation of Air Preheat Temperature

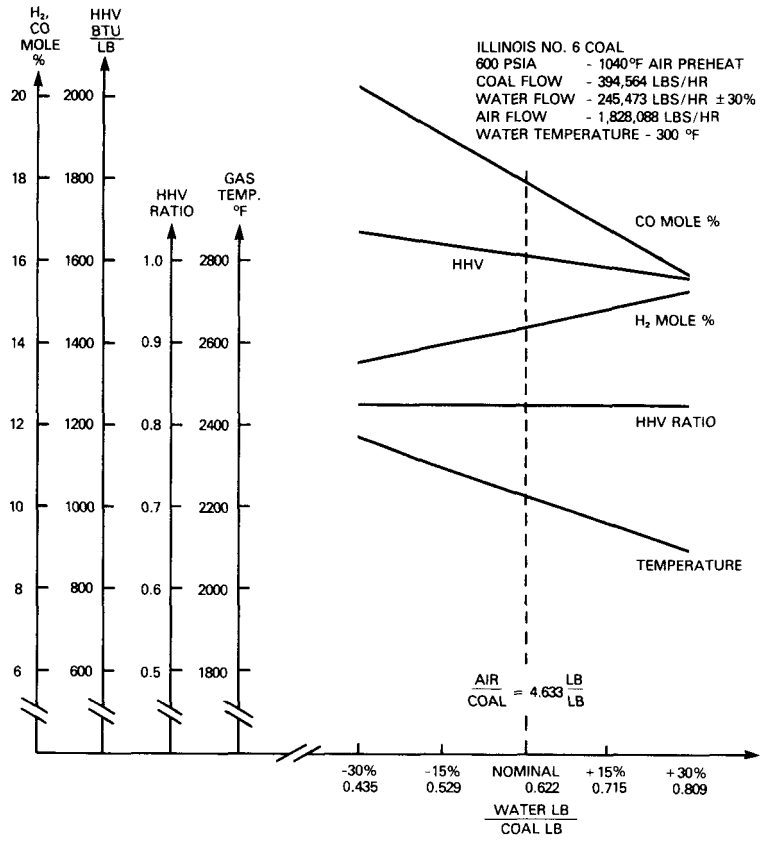

Figure 5-11. **Gasifier Variation of Water/Coal**

Table 5-5

COMPARISON OF AUTOTHERMAL
REFORMER MODEL

Product Gases	Model	Catalytica (8)
H_2	28.35	28.44
H_2O	20.03	19.79
CO	13.60	13.04
CO_2	6.73	7.18
CH_4	.01	0.10
N_2	30.96	31.43
H_2S	0.00	0.02
A_R	.32	0.0

Inputs

Oil (1100 ^oF)	1890 #/hr (H.V. = 19502.6 B/#)
Steam (1100 ^oF)	3696 #/hr
Air (1100 ^oF)	7724 #/hr
Pressure	55 psia

REFERENCES

1. Fuel Cell Research on Second-Generation Molten Carbonate Systems: Vol. I, Cell Performance as a Function of Feed-Gas Quality. Prepared by Institute of Gas Technology for Argonne National Laboratory under Contract No. 31-109-38-3552 (Project 8984 Final Status Report for period 1 July 1976 through 30 September 1977).

2. Development of Molten Carbonate Fuel Cells for Power Generation. Prepared by General Electric Company for DoE under Contract No. EC-77-C-03-1479 (Report No. SRD-78-086, Quarterly Progress Report 15 February 1978 through 15 May 1978).

3. "Integrated Coal Gasifier/Molten Carbonate Fuel Cell Power Plant Conceptual Design and Implementation Assessment." Energy Conversion Alternatives Study (ECAS), United Technologies Phase II Final Report, Report No. FCR-0237.

4. D.R. Cruise. "Notes on the Rapid Computation of Chemical Equilibria." Journal of Physical Chemistry, Vol. 68, No. 12, December 1964.

5. D.R. Cruise. "Information Manual for the Theoretical Propellant Evaluation Program (PEP IV)." December 1964 to present, Naval Weapons Center, China Lake, Cal.

6. JANAF Thermochemical Tables. The Dow Chemical Co., Midland, Mich.

7. Letter. Texaco Development Corporation to General Electric Company, June 20, 1977.

8. Catalytica Associates Inc. Assessment of Fuel Processing Alternatives for Fuel Cell Power Generation. EPRI Report EM-570, September 1977.